

The eye, the kidney, and cardiovascular disease: old concepts, better tools, and new horizons

Tariq E. Farrah^{1,2}, Baljean Dhillon^{3,4}, Pearse A. Keane⁵, David J. Webb¹ and Neeraj Dhaun^{1,2}

OPEN

¹University/BHF Centre for Cardiovascular Science, The Queen's Medical Research Institute, University of Edinburgh, Edinburgh, UK;

²Department of Renal Medicine, Royal Infirmary of Edinburgh, Edinburgh, UK; ³Centre for Clinical Brain Sciences, University of Edinburgh, Edinburgh, UK; ⁴Princess Alexandra Eye Pavilion, Edinburgh, UK; and ⁵NIHR Biomedical Research Centre for Ophthalmology, Moorfields Eye Hospital, London, UK

Chronic kidney disease (CKD) is common, with hypertension and diabetes mellitus acting as major risk factors for its development. Cardiovascular disease is the leading cause of death worldwide and the most frequent end point of CKD. There is an urgent need for more precise methods to identify patients at risk of CKD and cardiovascular disease. Alterations in microvascular structure and function contribute to the development of hypertension, diabetes, CKD, and their associated cardiovascular disease. Homology between the eye and the kidney suggests that noninvasive imaging of the retinal vessels can detect these microvascular alterations to improve targeting of at-risk patients. Retinal vessel-derived metrics predict incident hypertension, diabetes, CKD, and cardiovascular disease and add to the current renal and cardiovascular risk stratification tools. The advent of optical coherence tomography (OCT) has transformed retinal imaging by capturing the chorioretinal microcirculation and its dependent tissue with near-histological resolution. In hypertension, diabetes, and CKD, OCT has revealed vessel remodeling and chorioretinal thinning. Clinical and preclinical OCT has linked retinal microvascular pathology to circulating and histological markers of injury in the kidney. The advent of OCT angiography allows contrast-free visualization of intraretinal capillary networks to potentially detect early incipient microvascular disease. Combining OCT's *deep imaging* with the analytical power of deep learning represents the next frontier in defining what the eye can reveal about the kidney and broader cardiovascular health.

Kidney International (2020) ■, ■-■; <https://doi.org/10.1016/j.kint.2020.01.039>

KEYWORDS: chronic kidney disease; hypertension; imaging; microcirculation; ocular; proteinuria

Copyright © 2020, International Society of Nephrology. Published by Elsevier Inc. This is an open access article under the CC BY-NC-ND license (<http://creativecommons.org/licenses/by-nc-nd/4.0/>).

Correspondence: Neeraj Dhaun, Univeristy/BHF Centre for Cardiovascular Science, The Queen's Medical Research Institute, 47 Little France Crescent, Edinburgh, UK. E-mail: bean.dhaun@ed.ac.uk

Received 10 September 2019; revised 9 January 2020; accepted 13 January 2020; published online 27 February 2020

Chronic kidney disease (CKD) affects ~10% of the world's population, and its incidence is increasing.¹ Hypertension and diabetes mellitus are also common worldwide, with an estimated prevalence of ~30% and ~10%, respectively; both are important risk factors for the development and progression of CKD.^{2,3} These systemic diseases are strongly associated with incident cardiovascular disease (CVD), and their interrelationship contributes to CVD being the most common end point of CKD.⁴ The current clinical tools lack precision to detect, stratify, and track individual patients at increased risk of progressive CKD and CVD, and before end-organ damage. Thus, there is an urgent unmet need for simple noninvasive methods to allow earlier identification and risk stratification of patients at increased risk of progressive end-organ injury and subsequent end-stage renal disease and CVD.

Microvessels (luminal diameter <300 μm) regulate tissue perfusion and contribute to systemic vascular resistance. This ability is closely linked to endothelial function. Several pathophysiological processes may contribute to *and* be a consequence of endothelial dysfunction, with downstream effects on microvessels (Figure 1).⁵ Alterations in microvascular structure and function contribute to the development and progression of hypertension, diabetes, CKD, and CVD.⁵⁻⁷ Importantly, such changes precede the development of end-organ damage⁸ and appear modifiable.⁹ Moreover, microvascular dysfunction in peripheral beds mirrors dysfunction in visceral beds,^{10,11} providing a rationale for imaging accessible microvessels, such as those of the eye. Transparency of the ocular media allows direct visualization of the microvasculature that may be affected by systemic diseases such as hypertension, diabetes, and CKD. Here, we discuss the basis for the eye to act as a window to the kidney and evidence for the microcirculation of the eye to report risk of adverse renal and CVD outcomes.

THE EYE AS A WINDOW TO THE KIDNEY

The eye and kidney have several structural, developmental, and organizational similarities that support the concept that ocular tissues might reflect renal disease (Figure 2).

Bruch's membrane and glomerular basement membrane

Bruch's membrane divides the posterior pole of the eye into the retina (a laminated neurovascular structure) and choroid

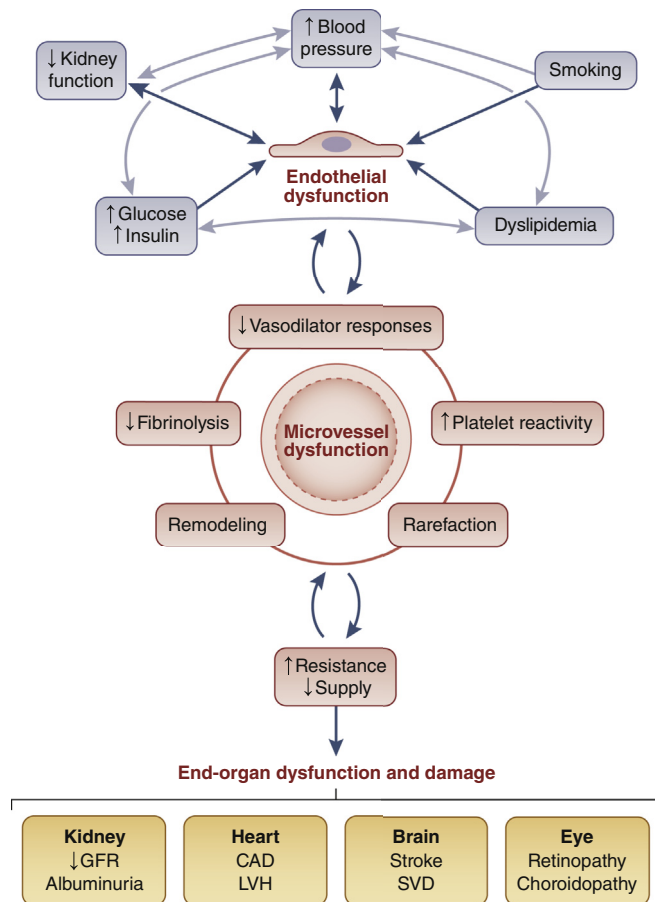


Figure 1 | Initiation and consequences of microvascular disease.⁵ Light blue arrows show the additional associations/contribution between insults. Dark blue arrows indicate the sequence of events leading to the development and progression of end-organ dysfunction. CAD, coronary artery disease; GFR, glomerular filtration rate; LVH, left ventricular hypertrophy; SVD, small vessel disease.

(an almost entirely vascular structure), collectively termed *chorioretinal*. Bruch's membrane and the glomerular basement membrane (GBM) both contain a network of $\alpha 3$, $\alpha 4$, and $\alpha 5$ type IV collagen chains.^{12,13} Thus, inherited or acquired diseases involving type IV collagen can affect both organs; the presence of coexistent nephropathy and retinopathy in Alport syndrome is a well-described example of this (Supplementary Figure S1).^{14,15} As another example, anti-GBM disease is characterized by the development of IgG autoantibodies directed against the $\alpha 3$ chain, which are deposited on glomerular and alveolar basement membranes triggering a crescentic glomerulonephritis and pulmonary hemorrhage, respectively.¹⁶ Similar linear IgG deposition on Bruch's membrane has been reported in patients with anti-GBM disease who developed concurrent choroidal ischemia and retinal detachment.^{17,18}

The arrangement of the choroidal capillary (choriocapillaris) endothelium, Bruch's membrane, and retinal pigment epithelium mirrors that of the glomerular

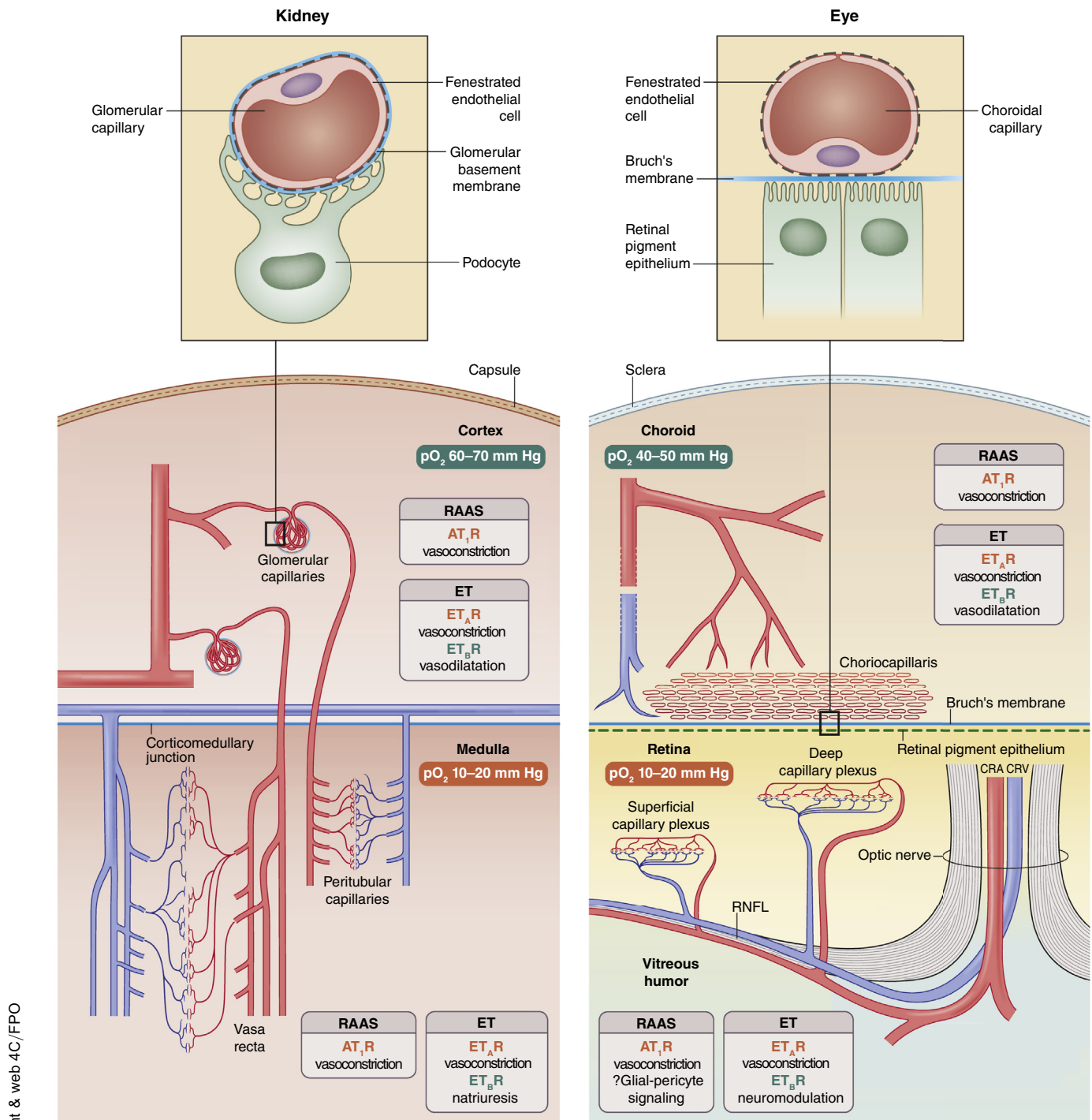
endothelium, GBM, and podocyte (Figure 2). The pathological relevance of this homology is readily appreciated in membranoproliferative glomerulonephritis type II, in which electron dense deposits are found on the GBM and on Bruch's membrane.¹⁹ Evidence of complement system dysregulation as a key driver of renal and retinal deposit formation in membranoproliferative glomerulonephritis²⁰ and drusen deposition on Bruch's membrane in age-related macular degeneration has extended the link between the eye and the kidney to include immune regulation.^{21,22}

Chorioretinal and renal microcirculations

Development and ultrastructure. The human retinal circulation develops predominantly by angiogenesis, where new vessels bud from preexisting ones, to supply the inner two-thirds of the retina.²³ In the kidney, the peritubular capillaries and vasa recta populate the medulla and inner cortex in a similar manner.²⁴ In contrast, the choroidal and glomerular endothelium is reported to develop by vasculogenesis, where clusters of progenitor cells form islands of *de novo* vessels, giving rise to the choriocapillaris and renal corpuscle, respectively^{24,25}; although for the glomerulus, this is debated.²⁶ The choriocapillaris endothelium has ~80 nm fenestrations allowing fluid exchange within the subretinal space.²⁷ The glomerular endothelium has similarly sized fenestrations that facilitate ultrafiltration into the Bowman's capsule.²⁸

Organization and blood flow. The retinal and medullary circulations each receive <20% of the total ocular and renal blood flow, respectively, despite the high metabolic activity of the retinal photoreceptors and the medullary countercurrent exchange system. Thus, both regions have a lower oxygen tension than do their choroidal and cortical counterparts, creating matched chorioretinal and corticomedullary oxygen gradients (Figure 2). The choroidal circulation receives ~80% of ocular blood flow and passively oxygenates key visual apparatus including the pigment epithelium and photoreceptors, particularly within the avascular fovea.²⁵ This role demands blood flow that is 4-fold higher per unit mass than the kidney and 10-fold higher than the brain,²⁵ indicating the importance of the choroid to global retinal health. Choroidal vascular change may therefore predate the onset of overt retinopathy and, if detectable, might allow earlier identification of incipient disease.

Regulation of blood flow. All components of the renin-angiotensin-aldosterone system are widely expressed throughout the retinal and choroidal vascular networks (Figure 2).²⁹ Similar to effects in the kidney, angiotensin II acting via type I receptors leads to chorioretinal vasoconstriction³⁰ but may also modulate glial-pericyte-vasomotor signaling that maintains retinal neurovascular integrity.³¹ Excessive renin-angiotensin-aldosterone system activation contributes to the pathogenesis of diabetic retinopathy and both diabetic and nondiabetic CKD.³² Moreover, renin-angiotensin-aldosterone system inhibition in clinical trials



print & web 4C/FPO

Figure 2 | The eye as a window to the kidney. The microcirculation of the eye and kidney are characterized by multiple capillary networks, which, although arranged in close proximity, have striking structural and functional differences. (a) Upper panel: cross-sectional diagram of the glomerular capillary. Lower panel: corticomedullary microcirculation organization, oxygen gradients, and actions of renal-angiotensin-aldosterone and endothelin systems. (b) Upper panel: cross-sectional diagram of the choroidal capillary. Lower panel: chorioretinal microcirculation organization, oxygen gradients, and actions of renal-angiotensin-aldosterone and endothelin systems. ?Glial-pericyte signaling, glial-pericyte signaling not proven; AT₁R, angiotensin II type 1 receptor; CRA, central retinal artery; CRV, central retinal vein; ET, endothelin; ET_AR, endothelin type A receptor; ET_BR, endothelin type B receptor; pO₂, partial pressure of oxygen; RAAS, renin-angiotensin-aldosterone system; RNFL, retinal nerve fiber layer.

prevents the development and progression of diabetic retinopathy and nephropathy, probably independently of effects on blood pressure (BP).³²

In the eye, endothelin-1 mediates vasoconstriction via endothelin-A receptors, which are predominantly localized to choroidal and retinal vascular smooth muscle cells. In

contrast, endothelin-B receptors appear confined to neuronal and glial structures.³³ Similarly in the kidney, endothelin-A receptors are localized to the vascular smooth muscle of glomeruli and vasa recta whereas endothelin-B receptors are mainly localized to the collecting system (Figure 2). Selective endothelin-A receptor blockade in the eye increases retinal blood flow and reduces both retinal pericyte apoptosis and retinal thinning in a mouse model of type 2 diabetes.³⁴ These effects are mirrored in the kidney where selective endothelin-A blockade ameliorates intraglomerular hypertension, podocytopeny, and fibrosis to slow CKD progression.^{35,36} Autonomic innervation in the eye is limited to the choroidal circulation where sympathetic activation mediates choroidal vasoconstriction²⁵ in a similar manner to effects on intrarenal vessels. Thus, the choroidal microvasculature, rather than retinal vessels, may more accurately reflect the renal microvasculature, particularly in diseases characterized by excessive sympathetic activation, such as CKD.¹

RETINAL IMAGING, THE KIDNEY, AND CVD

Retinal photography

Qualitative retinopathy grading (e.g., microaneurysms, hemorrhages, or focal arteriolar narrowing) and computer-assisted quantitative retinal vessel caliber analysis of digital fundus photographs have been the mainstay of retinal imaging for the last 20 years (Supplementary Figure S2). As retinopathy reflects established end-organ damage, detecting changes in retinal vessel caliber that precede this overt damage may allow earlier identification of at-risk patients.³⁷ The most established metrics are derived from arteriolar and venular widths from vessels close to the optic disc (Table 1; Supplementary Figure S2). Novel indices of retinal vascular network geometry, such as fractal dimension (*Dfs*), can be derived from skeletonized vessel maps from retinal photographs (Figure 3). These indices identify suboptimal vascular branching patterns that may reflect and promote microvascular damage in systemic disease.^{38,39} The presence and severity of retinopathy, vessel caliber change, and fractal deviations have been strongly linked to hypertension, diabetes mellitus, and CKD as well as CVD end points.

The retinal circulation: CVD risk factors and outcomes

Hypertension. Retinal arteriolar narrowing is thought to reflect increased systemic vascular tone. Large cross-sectional studies demonstrate strong independent associations between BP and generalized and focal arteriolar narrowing.⁴⁰ Longitudinal studies have shown that retinal arteriolar narrowing is associated with a ~2-fold increased risk of incident hypertension independent of age, sex, baseline BP, and other CVD risk factors (Supplementary Table S1), supporting the concept that retinal microvascular changes precede overt disease and are able to identify at-risk individuals. This paradigm has been challenged more recently by data suggesting a high prevalence of masked hypertension at the time of retinal imaging as detected by ambulatory BP monitoring.⁴¹

Additionally, systolic BP and mean arterial pressure show an inverse linear relationship with *Df* in keeping with rarefaction.^{42–44} This relationship holds true in young children with normal BP (a population that should lack confounding pre-existing vascular risk factors) and is independent of retinal arteriolar caliber.⁴⁵

Diabetes mellitus. Diabetic retinopathy is associated with systemic vascular complications likely reflecting widespread microvascular disease.⁷ More so than in hypertension, retinal venular widening is prevalent in diabetes, correlates with the severity of retinopathy, and predicts progression to overt retinopathy, suggesting a different pathophysiological basis for the change in vessel caliber.⁴⁶ Wider venules are seen in response to chronic hypoxia⁴⁷ and associate with endothelial dysfunction,⁴⁸ suggesting that they reflect microvascular stress in response to metabolic derangement. In support of this concept, higher cholesterol level, higher body mass index, and worse glycemic control link to wider retinal venules.^{49–52} Moreover, wider venules and smaller arteriole-to-venule ratio predict incident fasting hyperglycemia and diabetes over 5 to 10 years, independent of fasting glucose level, insulin level, body mass index, family history of diabetes, or BP (Supplementary Table S2).⁵³ Finally, reduced *Df* in those with diabetes can predict incident neuropathy, nephropathy, and progressive retinopathy, independent of other risk factors for microvascular complications although the strength of these associations is modest.^{54,55}

CKD. Retinopathy (diabetic, hypertensive, or otherwise) is more prevalent in patients with CKD, independent of standard CVD risk factors including diabetes and proteinuria.⁵⁶ Retinopathy severity also shows a graded relationship with declining estimated glomerular filtration rate (eGFR) and its presence predicts future decline in renal function.^{57,58} Analysis of ~1000 patients from the Chronic Renal Insufficiency Cohort with serial fundus photographs found that retinopathy progression also tracks CKD progression in a subgroup of patients.⁵⁹ However, these initial associations were lost after adjusting for baseline risk factors for progression, suggesting little added benefit of retinal metrics.⁵⁹ Both arteriolar narrowing and venular widening have been associated with prevalent CKD,⁶⁰ but whether retinal vessel calibers predict incident or progressive CKD is not clear (Table 2). The Atherosclerosis Risk in Communities Study examined retinal photographs of ~10,000 middle-aged patients and showed that those in the lowest arteriole-to-venule ratio quintile had the greatest increase in serum creatinine level over a 6-year period; this held true after adjusting for baseline vascular risk factors.⁵⁸ Analysis of retinal images from ~4500 patients without baseline CKD from the Multi-Ethnic Study of Atherosclerosis found that narrower arterioles predicted the development of CKD in white patients alone.⁶⁴ However, other large well-designed studies have failed to find an independent association between any vascular caliber metric and CKD progression.^{60,63}

Albuminuria, an established marker of renal microvascular injury and an independent risk factor for CKD progression

Table 1 | Retinal vascular metrics from retinal photography

Metric	Derivation	Interpretation	Strengths	Weaknesses
CRAE	Widths of the reflective erythrocyte column within the vessel lumen from 6 largest arterioles located in a zone 0.5–1 disc diameters away from the optic disc margin	Summarized surrogate measure of internal arteriolar widths that reflect narrowing or widening	Provides insight into disease affecting arterioles Relatively easy to obtain and automate	Summarized rather than absolute values Potential for magnification and positioning errors Values are not true vessel widths nor cross-sectional area that may be more relevant to disease
CRVE	Widths of the reflective erythrocyte column within the vessel lumen from 6 largest venules located in a zone 0.5–1 disc diameters away from the optic disc margin	Summarized surrogate measure of internal venular widths that reflect narrowing or widening	Provides insight into disease affecting venules Relatively easy to obtain and automate	Summarized rather than absolute values Potential for magnification and positioning errors Values are not true vessel widths nor cross-sectional area that may be more relevant to disease
AVR	Ratio of CRAE to CRVE	Changes usually indicative of generalized arteriolar narrowing	Avoids magnification errors Dimensionless	Provides little insight into the underlying pathophysiology If used alone, it can lead to incorrect inferences: both CRVE and CRAE narrow with increasing blood pressure, producing a normal AVR masking any association
<i>Df</i>	Images are binarized and vessel maps are broken into short segments (<i>skeletonization</i>) Entire image divided into boxes, and those containing a vessel segment are counted. The process is repeated with different box sizes. The number of boxes with vessel segments is plotted against the total number of boxes in the image	Index of vessel network spatial occupancy (complexity) Reduced (sparse) or increased (dense) complexity relative to health or within a cohort reflects suboptimal vascular network geometry	Based on robust models of the optimality of vascular branching May be more sensitive than calibers in reflecting microvascular disease in other organ beds	Less widely studied than calibers Simplifies 3-dimensional vascular networks into 2-dimensional skeletonized maps

AVR, arteriole-to-venule ratio; CRAE, central retinal arteriolar equivalent; CRVE, central retinal venular equivalent; *Df*, fractal dimension.

and incident CVD,¹ may better reflect retinal vascular changes. Cross-sectional studies have shown that a narrower central retinal arteriolar equivalent is independently associated with higher albuminuria⁷⁰ and more severe glomerulopathy on histology in early diabetic CKD,⁷¹ linking retinal and renal microvascular pathology. Additionally, baseline and subsequent arteriolar narrowing predicts worsening albuminuria and histological disease progression as well as decline in eGFR in both diabetic and nondiabetic CKD.^{61,65,71} Importantly, using central retinal arteriolar equivalents in conjunction with albuminuria allowed better stratification of individuals at increased risk of CKD progression than did the use of albuminuria alone.⁶⁵

Studies exploring fractals in CKD are few and conflicting. A small study from Singapore (n = 260) found a modest U-shaped relationship between *Df* and CKD, suggesting that increased vascular branching complexity, potentially due to neovascularization as is often seen in diabetic retinopathy, is also indicative of increased risk.⁷² A larger Malay study (n = 3280) subsequently found lower *Df* to be strongly associated with lower eGFR and higher proteinuria.⁷³ In contrast, large studies of both diabetic and nondiabetic CKD found no

relationship between either baseline or change in *Df* and the presence or progression of CKD (Table 2).^{69,74}

The lack of a consistent retinal vascular metric for the detection of incident and prevalent CKD may reflect the heterogeneity of the study populations, underlying etiologies, metabolic abnormalities, and treatments, such as immunosuppression and erythropoietin-stimulating agents. It may also suggest that retinal photography has limited sensitivity to reveal a reliable metric among these competing influences.

CVD outcomes. Retinal arteriolar narrowing, in contrast to venular widening, shows stronger associations with atherothrombotic rather than metabolic CVD risk factors,⁵² but both link to CVD outcomes. Large epidemiological studies and meta-analyses have shown that retinopathy, narrower arterioles, and wider venules are common in patients with known ischemic stroke disease.^{75–77} Moreover, their presence predicts incident ischemic stroke and stroke mortality, independent of other baseline CVD risk factors (Supplementary Table S3).^{78–80} These same metrics are also independent predictors of atherosclerotic coronary artery disease morbidity and mortality, which appear stronger for women than men (Supplementary Table S3).^{81,82} A lower *Df*

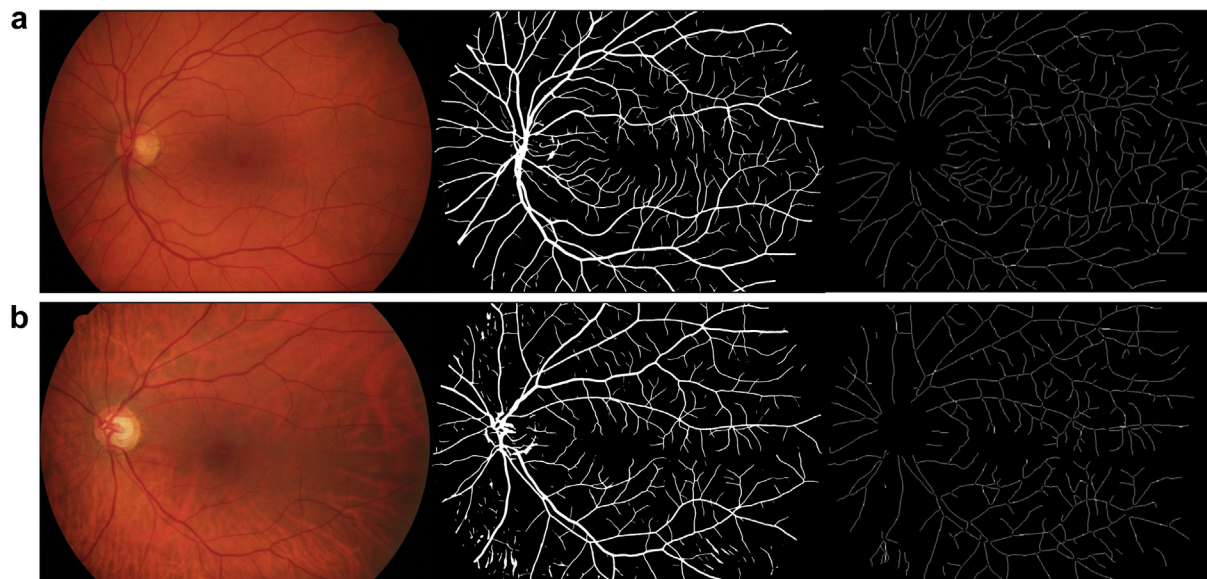


Figure 3 | Retinal vascular network geometric indices. Retinal photographs (left panels) of the left eye taken using the Canon CR-1 fundus camera (Canon Inc., Tokyo, Japan) with a field of view of 45° in (a) a healthy volunteer and (b) a patient with chronic kidney disease (CKD). Arterial and venous branches are binarized and segmented (middle panels) before being transformed into vessel (arterial) skeleton maps (right panels) for fractal dimension (D_f) analyses. The vessel segmentation and skeleton maps demonstrate retinal vessel rarefaction in CKD compared with health, which is not evident from the standard retinal photographs; health $D_{f_{\text{arteries}}} = 1.47$ and CKD $D_{f_{\text{arteries}}} = 1.18$. Retinal photographs and segmentation images used under Creative Commons license from <https://www5.cs.fau.de/research/data/fundus-images/>. Vessel skeleton map images kindly provided by Stephen Hogg (VAMPIRE group, University of Dundee, Dundee, UK). To optimize viewing of this image, please see the online version of this article at www.kidney-international.org.

showed a linear relationship with worsening severity of coronary vessel stenosis in ~ 1700 patients with ischemic heart disease⁸³ and also associated with prevalent stroke.⁸⁴ In large prospective studies, a suboptimal D_f conferred a 40% increased risk of stroke over a 5-year period⁸⁵ and a 50% increased risk of death from coronary artery disease over a 14-year period (Supplementary Table S3).⁸⁶ These analyses included adjustment for standard CVD risk factors and retinal vessel calibers, suggesting a better predictive ability of D_f .⁸⁶

The presence of retinal microvascular disease may also stratify patients at future risk of CVD as demonstrated by a recent study of >3500 patients with microalbuminuria. Here, a wider central retinal venular equivalent predicted incident CVD over 6 years.⁸⁷ Furthermore, the presence of a single retinal microvascular abnormality, in conjunction with microalbuminuria, increased the risk of incident CVD 2-fold, and this rose to >6 -fold if multiple vascular abnormalities were present.⁸⁷ Finally, and importantly, the use of retinal vascular metrics such as arteriolar narrowing and venular widening can provide added benefit over current atherosclerotic CVD risk prediction tools as demonstrated for ischemic stroke⁸⁰ and coronary artery disease.⁸⁸

These data provide robust evidence of the potential clinical utility of retinal imaging-based CVD risk assessment. Transition into clinical practice is still awaited and may have been hindered by inherent limitations (Table 1). The use of novel imaging modalities to target deeper vascular networks such as

the choroidal circulation, which may reflect microvascular disease earlier and more accurately, might overcome some of these challenges. This is now possible through retinal optical coherence tomography (OCT).

Retinal OCT

Retinal OCT provides high-resolution tomographic (cross-sectional) imaging of the eye with near histological detail.⁸⁹ The advent of retinal OCT has transformed clinical ophthalmology. In 2010, an estimated 16 million OCT scans were performed in the United States alone, more than all other ocular imaging modalities combined.⁹⁰ This rapid expansion has provided novel insights into the role of the chorioretinal microvasculature in the pathogenesis of age-related macular degeneration, diabetic retinopathy, and glaucoma, eye diseases that have an increased prevalence in CKD.⁶⁰ The technical principles underpinning OCT are analogous to those of ultrasound but measure light reflections rather than sound echoes (Supplementary Figure S3). The measurement of small variations (interference) in light waves over short distances is made possible through the use of interferometry. In the current generations of OCT, a Fourier transform analyzes multiple interference signals simultaneously via a spectrometer (spectral domain OCT) or a tunable laser (swept-source OCT), resulting in extremely fast image acquisition.⁸⁹ Swept-source OCT may also provide better tissue penetration than does spectral domain OCT,

Table 2 | Retinal vascular metrics to predict incident or progressive CKD

Study	Country	N	Population and mean age	Retinal metric	Clinical outcome	Hypertension	Mean BP	Diabetes	Index serum creatinine level or eGFR	Follow-up duration	Results
Wong <i>et al.</i> ⁵⁸ Prospective population-based cohort	United States	10,056	White and African American adults with eGFR >60 ml/min per 1.73 m ² 60 yr	AVR	Incident renal dysfunction: rise in serum creatinine level by ≥ 35 $\mu\text{mol/l}$ or hospital admission/death coded for renal disease	50%	127/70 mm Hg	22%	80 $\mu\text{mol/l}$	6 yr	3% developed CKD Smallest AVR associated with a greater change in serum creatinine level (4 $\mu\text{mol/l}$ vs. 2 $\mu\text{mol/l}$)
Wong <i>et al.</i> ⁶¹ Prospective population-based cohort	United States	557	Type 1 diabetic patients with eGFR >90 ml/min per 1.73 m ² and proteinuria <0.3 g/l 31 yr	CRAE CRVE	Incident renal insufficiency: eGFR <60 ml/min per 1.73 m ² Incident gross proteinuria: >0.3 g/l	No data	120/76 mm Hg	100%	No data	16 yr	20% developed CKD 33% developed proteinuria Widest CRVE quartile associated with the increased incidence of CKD and proteinuric CKD: adjusted RR 1.5 (1.05–2.2) Proteinuria: adjusted RR 1.5 (1.2–2.0) No association for CRAE
Edwards <i>et al.</i> ⁶² Prospective population-based cohort	United States	1394	Adults aged >65 yr 78 yr	AVR	Change in serum creatinine level Decline in renal function: increase in serum creatinine level by ≥ 27 $\mu\text{mol/l}$ and fall in eGFR by $\geq 20\%$	57%	131/67 mm Hg	17%	89 $\mu\text{mol/l}$ 70 ml/min	4 yr	4%–5% had a significant increase in serum creatinine level or fall in eGFR AVR showed no associations with changes in renal function Retinopathy associated with a higher risk of decline in renal function: adjusted OR 2.8–3.2 vs. no retinopathy
Sabanayagam <i>et al.</i> ⁶³ Prospective population-based cohort	United States	3199	White adults with eGFR >60 ml/min per 1.73 m ² 59 yr	CRAE CRVE	Incident CKD: eGFR <60 ml/min per 1.73 m ² and 25% decrease from baseline	45%	130/78 mm Hg	9%	85 ml/min	15 yr	5% developed CKD No association of CRAE or CRVE with incident CKD No association with eGFR and incident CRAE narrowing or CRVE widening
Yau <i>et al.</i> ⁶⁴ Prospective population-based cohort	United States	4594	Multi-ethnic adults with eGFR >60 ml/min per 1.73 m ² 64 yr	CRAE CRVE	Incident CKD: eGFR <60 ml/min per 1.73 m ²	40%	127/71 mm Hg	11%	76 ml/min	4.8 yr	5% developed CKD Narrowest CRAE tertile associated with incident CKD in <i>white patients only</i> : adjusted HR 1.78 (1.01–3.1) vs. widest; increased to 2.95 when analyzing those without hypertension or diabetes
Baumann <i>et al.</i> ⁶⁵ Prospective	Germany	141	Adults with stage 2–4 CKD 61 yr	CRAE	Progression of CKD: 50% decline in eGFR or start of RRT	No data	137/76 mm Hg	46%	48 ml/min	3.9 yr	No association with CRVE 17% had progression of CKD Narrowest CRAE tertile associated with progression of CKD: adjusted OR 3 (1.2–7.5) vs. widest CRAE Narrowest CRAE in the presence of albuminuria associated with a 10-fold increased risk of CKD progression as

(Continued on next page)

8 **Table 2 | (Continued) Retinal vascular metrics to predict incident or progressive CKD**

Study	Country	N	Population and mean age	Retinal metric	Clinical outcome	Hypertension	Mean BP	Diabetes	Index serum creatinine level or eGFR	Follow-up duration	Results
Grunwald <i>et al.</i> ⁶⁶ Prospective population-based cohort	United States	1852	Adults with eGFR 20–70 ml/min per 1.73 m ² 62 yr	AVR CRAE CRVE	Progression of CKD: ESRD/RRT, change in eGFR slope	90%	130/80 mm Hg	47%	40 ml/min	2.3 yr	compared with a 3-fold risk seen with narrow CRAE or albuminuria alone 8% developed ESRD and overall eGFR decline was 0.53 ml/min per 1.73 m ² Higher AVR associated with ESRD and steeper eGFR decline: adjusted HR 3.1 (1.5–6.4) No associations with CRAE and CRVE
Yip <i>et al.</i> ⁶⁷ Prospective population-based cohort	Singapore	5763	Malay adults 55 yr	AVR CRAE CRVE <i>Df</i>	Incident ESRD: defined by start of RRT	55%	140/70 mm Hg	34%	77 ml/min	4.3 yr	0.4% developed ESRD No associations for vascular metrics and the risk of ESRD in adjusted analyses Retinopathy predicted ESRD
Yip <i>et al.</i> ⁶⁸ Prospective population-based cohort	Singapore	1256	Malay adults 56 yr	CRAE CRVE Tortuosity <i>Df</i> Branching angles	Incident CKD: eGFR <60 ml/min per 1.73 m ²	58%	150/80 mm Hg	25%	80 ml/min	6 yr	6% developed incident CKD Narrower CRAE associated with incident CKD: adjusted HR 1.3 (1.00–1.78) as a continuous variable Widest CRVE tertile associated with incident CKD: adjusted HR 2.4 (1.1–5.9) vs. narrowest CRVE No other vascular metrics associated with incident CKD
McKay <i>et al.</i> ⁶⁹ Prospective population-based cohort	Scotland	1068	Adults with eGFR ≥60 ml/min per 1.73 m ² 63 yr	CRAE CRVE Tortuosity <i>Df</i> Branching angles	Change in eGFR: <i>Progressors</i> : eGFR <60 ml or ≥15% decline <i>Nonprogressors</i> : <10% decline	No data	138/77 mm Hg	100%	94 ml/min	3 yr	31% had <i>progressive</i> CKD No baseline retinal metric predicted progression of CKD in unadjusted or adjusted analyses

AVR, arteriole-to-venule ratio; BP, blood pressure; CKD, chronic kidney disease; CRAE, central retinal arteriolar equivalent, CRVE, central retinal venular equivalent; *Df*, fractal dimension; eGFR, estimated glomerular filtration rate; ESRD, end-stage renal disease; HR, hazard ratio; OR, odds ratio; RR, risk ratio; RRT, renal replacement therapy. All values are mean.

wing better identification of deep structures such as the choroid.⁹¹

The ultrahigh resolution (typically 2–8 μm) of OCT allows identification and automated segmentation of retinal layers, providing measures of global and regional retinal thickness, volume, and nerve fiber layer thickness, allowing detection of retinal neurodegeneration (Table 3 and Figure 4; Supplementary Figure S4 and Supplementary Movies S1 and S2).⁸⁹ Importantly, OCT devices are capable of eye tracking and image coregistration for accurate longitudinal imaging. Another key strength of OCT is the potential to image the previously inaccessible choroid, which is almost entirely composed of the blood vessels of the choroidal circulation (Figure 4). OCT-derived metrics of choroidal structure have been shown to be reproducible, correlate well with histology, and may be surrogate measures for microvascular density with thinning, suggestive of rarefaction.^{92–94} In addition, the cross-sectional nature of the OCT image allows vessel wall/lumen analyses. OCT devices can also acquire *en face* retinal images for vessel caliber assessment to complement choroidal imaging (Supplementary Figure S2).⁹⁵ In short, OCT allows comprehensive structural assessment of the entire chorioretinal circulation and its dependent tissue *in vivo* within a single platform.

The chorioretinal circulation: CVD risk factors and outcomes

Hypertension. We have used OCT to prospectively examine chorioretinal thickness in patients with established hypertension and age- and sex-matched healthy subjects.⁹⁶ We excluded patients with a history of eye disease, diabetes, or overt CVD. We found no differences in OCT metrics between these carefully matched groups. Two larger studies have produced contrasting results. The Beijing Eye Study imaged ~ 3000 adults and reported small increases in choroidal thickness with increasing diastolic BP but not systolic BP.⁹⁷ Paradoxically, the presence of hypertension was characterized by choroidal thinning. A subsequent cross-sectional study from Korea found that patients with hypertension ($n = 140$) had significant retinal thinning in nearly all regions assessed as compared with those without hypertension ($n = 687$).⁹⁸ Notably, the hypertensive group was older with a higher prevalence of CVD risk factors. More recently, a single-center study from Italy of 100 patients with hypertension found consistent retinal and choroidal thinning in hypertensive patients with coexistent CKD (defined as an eGFR < 60 ml/min per 1.73 m² and/or moderate albuminuria) as compared with hypertensive patients with preserved renal function.⁹⁹ These differences persisted after adjustments for age, antihypertensive use, and glycemia. The lack of a matched healthy control group in this otherwise well-designed study limits wider generalizability to CVD risk.

OCT also enables cross-sectional assessment of retinal vessels. Muraoka *et al.* reported a greater arteriolar and venular wall thickness in 106 hypertensive patients than in 132 patients without hypertension.¹⁰⁰ Given that the lumen size

remained normal, the findings of Muraoka *et al.* suggested outward vascular remodeling.

Interpreting the broader significance of these contrasting results in hypertension is difficult as different ethnic groups were studied, imaging devices were varied, medication and comorbidity data were inconsistently reported, and those with diabetes were variably included. Large prospective studies that take such factors into account are needed to clarify any relationship and explore causality.

Diabetes mellitus. The studies using OCT to assess retinal thickness between patients with and without diabetes overall have shown significant thinning of the nerve fiber and ganglion cell layers (GCLs) even when retinopathy is absent or mild.^{101–103} Retinal ganglion cells are interneurons that transmit visual information from photoreceptor cells to the visual cortex via the optic nerve. Ganglion cell apoptosis is an early hallmark of retinal neurodegeneration that manifests as thinning of the GCL on OCT.¹⁰⁴ Such GCL thinning is not observable by standard retinal photography or scanning laser ophthalmoscopy.¹⁰⁴ Studies using OCT in types 1 and 2 diabetes, with no or minimal clinically observable retinopathy, have found selective GCL thinning as compared with health.^{101,102} The degree of thinning correlates strongly with the duration of type 1 diabetes.¹⁰¹ Studies of the choroid also show that patients with diabetes have thinner choroids than do age- and sex-matched controls, even in the absence of retinopathy.^{105,106} Recent work suggests that greater reductions in choroidal thickness and choroidal vascular density occur with worsening retinopathy in keeping with progressive microvascular damage.¹⁰⁷ Whether choroidal thinning contributes to, or indeed is a result of, retinal vascular disease needs further study. The choroid may therefore reflect early systemic vascular changes in diabetes, such as glomerular hyperfiltration and hypertension.

Predialysis CKD. We showed, for the first time, that patients with varying degrees of nondiabetic predialysis CKD exhibit $\sim 5\%$ retinal and $\sim 25\%$ choroidal thinning as compared with both age- and sex-matched healthy subjects and patients with hypertension (Figure 4).⁹⁶ The highly vascular nature of the choroid suggests that thinning here is likely to represent changes in microvascular structure or function. Supporting this, we found that the choroid was thinner in those with a lower eGFR and higher proteinuria, both strongly associated with microvascular dysfunction.^{108,109} Also, those with a thinner choroid had higher circulating endothelin-1 and plasma asymmetric dimethylarginine (an endogenous inhibitor of nitric oxide synthesis) levels, further supporting this association. Importantly, we linked chorioretinal thinning with renal histology, showing that the severity of glomerular injury reflected the degree of choroidal thinning. Recent data using different OCT platforms have confirmed our results. The previously discussed Italian study found that lower eGFR and higher microalbuminuria were associated with choroidal thinning using swept-source OCT in 100 hypertensive patients.⁹⁹ Moreover, with respect to eGFR, this association was independent of age

Table 3 | Chortioretinal layer metrics from optical coherence tomography

Metric	Derivation	Interpretation	Strengths	Weaknesses
Retinal thickness	<p>Calculated from the number of A-scan pixels between the internal limiting membrane and Bruch's membrane</p> <p>Sequential A scans in the horizontal or vertical plane generate a 2-dimensional thickness profile across the retina: the B scan</p>	<p>Average thickness of peripheral and central retinal subfields</p> <p>Thinning predominantly reflects neuronal loss. May also reflect intraretinal capillary rarefaction</p> <p>Thickening reflects accumulation of edema, vascular exudates, or cellular debris</p>	<p>Can allow detection of differential patterns of retinopathy: global thinning vs. predominantly central or peripheral subfield thinning</p> <p>Easy to obtain, automated, and highly reproducible</p> <p>Segmentation of retinal sublayers can provide a novel insight into pathogenesis such as GC layer thinning</p>	<p>Layer and subfield boundaries not standardized across devices</p> <p>Overall thickness may miss sublayer thinning or thickening</p> <p>Cannot differentiate between neuronal or vascular structures</p>
Macular volume	<p>Calculated as a product of retinal thickness and scan area. The scan area can be subdivided into the Early Treatment Diabetic Retinopathy Study map of 6, 3, and 1 mm concentric rings centered on the fovea, producing 9 subfields</p>	<p>Global and regional volumes of the key region for vision</p> <p>Thinning predominantly reflects neuronal loss. May also reflect intraretinal capillary rarefaction</p> <p>Thickening reflects accumulation of edema, vascular exudates, or cellular debris</p>	<p>Can allow early detection and tracking of differential patterns of maculopathy</p> <p>Segmentation of sublayers can provide a novel insight into pathogenesis</p> <p>Easy to obtain, automated, and highly reproducible</p>	<p>Accuracy dependent on the total number of stacked horizontal B scans within the scan area</p> <p>Layer boundaries and B-scan protocols not standardized across devices</p>
RNFL thickness	<p>Calculated from the number of A-scan pixels between the internal limiting membrane and the GC layer</p> <p>Sequential A scans in the horizontal, vertical, or circular plane centered on the optic disc generate a thickness profile</p>	<p>Global and regional assessments of the GC axon number</p> <p>Thinning reflects GC axonal loss</p> <p>Thickening reflects axonal edema seen in inflammation, ischemia, or intracranial hypertension</p>	<p>Specific biomarker of optic neuropathy and wider central neurological disease</p> <p>Allows earlier detection and tracking of differential patterns of neuropathy</p> <p>Easy to obtain, automated, and highly reproducible</p> <p>Standardized normative range available for glaucoma and neurological disease</p>	<p>Blood vessels (and glial cells) within the RNFL are included in measurement, so not truly representative of the GC axon population</p> <p>Segmentation errors can occur</p> <p>Susceptible to confounding by optical biometrics such as axial length, disc size, and disc-fovea angle</p>
Choroidal thickness	<p>No precise definition or standard methodology. Calculated from the number of A-scan pixels from Bruch's membrane to the choroidoscleral interface</p> <p>Often manually measured at several discrete locations</p> <p>Newer devices provide automatic segmentation to automatically calculate regional choroidal thickness and volume in a manner similar to that for retinal thickness and volume</p>	<p>Coarse measure of a dense vascular layer containing arterioles, capillaries, venules, and veins</p> <p>Thinning reflects vascular changes including reduced blood flow, vasoconstriction, or rarefaction.</p> <p>Contribution of nonvascular components unclear</p> <p>Thickening may be due to increased blood flow, vasodilatation, or edema. Contribution of nonvascular components unclear</p>	<p>Easy to obtain, increasingly automated, and reproducible</p> <p>Assess critical vascular supply to the retina and reveals a novel insight into macular disease</p>	<p>Inaccessible location continues to limit comprehensive vascular assessment</p> <p>Does not differentiate between vascular and nonvascular structures</p> <p>Susceptible to confounding by optical biometrics such as axial length</p> <p>No standardized normative range</p>

GC, ganglion cell; RNFL; retinal nerve fiber layer.

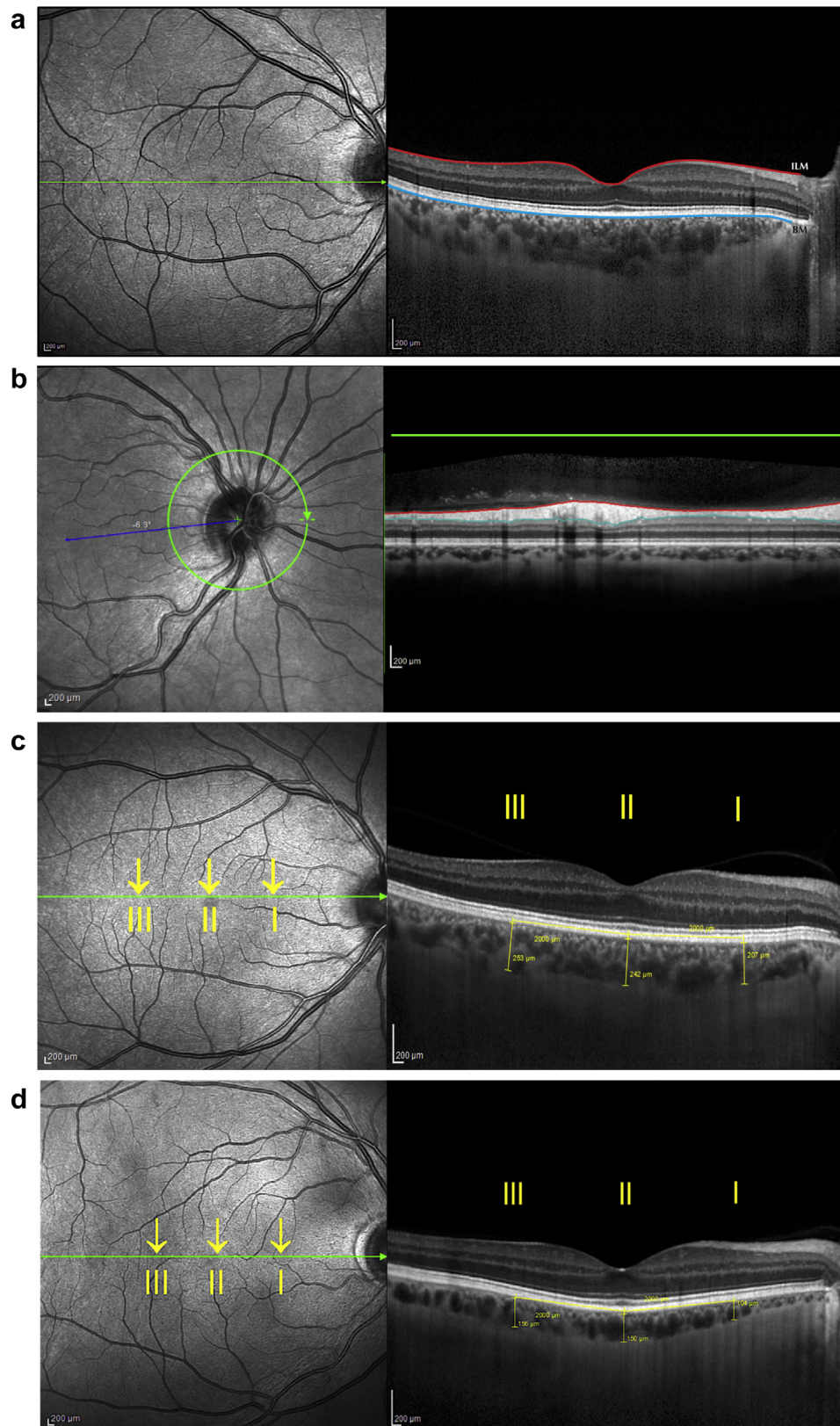


Figure 4 | Deep imaging with optical coherence tomography (OCT). *En face* confocal scanning laser ophthalmoscope (CLSO; left panels) and OCT (right panels) images of the right eye taken using the SPECTRALIS spectral domain OCT machine (SD-OCT; Heidelberg Engineering, Heidelberg, Germany) in (a–c) a healthy volunteer and (d) a patient with chronic kidney disease (CKD) with enhanced depth imaging (c,d). Bars = 200 μ m. (a) SD-OCT enables the identification of specific cell layers within the retina in high resolution. Left panel: an *en face* CLSO image centered over the macula. The green line represents the level and direction of the cross section of the corresponding OCT image running from left to right. Right panel: an OCT image demonstrating individual layers within the retina. *Retinal thickness* is defined (continued)

and other vascular risk factors.⁹⁹ These results are interesting as eGFR was preserved (~ 70 ml/min per 1.73 m²) and proteinuria was low, suggesting only modest microvascular damage. This contrasts with our work, where patients with CKD had moderate-to-severe renal disease (mean eGFR ~ 37 ml/min per 1.73 m²; proteinuria equivalent to ~ 2 g/d).⁹⁶ Another recent study included patients with more advanced CKD and found a consistent relationship between lower eGFR, higher protein leak, and a thinner choroid.¹¹⁰ The differences in OCT metrics between CKD, hypertension, and health, as well as their associations with CKD severity, provide the initial evidence of the potential of OCT to identify and stratify individuals at increased CVD risk. Whether these metrics reflect systemic microvascular damage better than standard tools should be tested in future studies. Finally, the consistency of these findings across different OCT devices using different technology and segmentation algorithms at least supports the fidelity of the relationship. Studies exploring whether this relationship can predict CKD outcomes are awaited.

End-stage renal disease. CVD risk is highest in those with end-stage renal disease and on maintenance dialysis.¹ Hemodialysis is associated with repetitive subclinical myocardial injury, which has been linked to microvascular dysfunction that likely contributes to this risk.¹¹¹ A simple noninvasive method of assessing microvascular disease in this very high risk group would be useful. In keeping with our data, studies have shown that patients on dialysis have global retinal thinning as compared with healthy controls.¹¹² Additionally, a few small clinical studies in these patients have assessed how OCT metrics may be influenced by dialysis *per se* (Table 4). Collectively, these studies suggest that the choroid, and the retina to a lesser extent, thins after dialysis, with the greatest reductions seen in patients with diabetic retinopathy. Whether thinning occurs because of changes in BP (altering chorioretinal perfusion), solute clearance, fluid removal, or change in intraocular pressure is unclear, and the studied cohorts are probably too small and/or heterogeneous to assess these relationships in detail. Retinal nerve fiber layer thinning has been associated with neurodegenerative disease such as Alzheimer disease and Parkinson disease,¹²⁵ suggesting that OCT can act as a window to the brain and cognition. Similar thinning has been found in patients on hemodialysis¹²⁴ and supports recent data linking intradialytic cerebral

hypoperfusion to progressive cognitive impairment.¹²⁶ There are no robust OCT studies in renal transplant recipients, but the available data suggest that retinopathy and nerve fiber layer thinning are common.¹²⁷

CVD outcomes. Studies linking OCT-derived metrics to prevalent CVD are beginning to emerge. Altinkaynak *et al.* studied 56 patients with heart failure with a reduced ejection fraction and found choroidal thinning of $\sim 30\%$ as compared with age- and sex-matched healthy controls.¹²⁸ A thinner choroid was strongly associated with a worse ejection fraction in unadjusted analyses, which may reflect choroidal vasoconstriction secondary to reduced cardiac output.¹²⁸ No data on possible confounders such as renal function, diabetic status, CVD risk factors, and concomitant drugs were reported.

Choroidal but not retinal thinning has been shown in patients with established coronary artery disease (defined by angiographic coronary artery stenosis, a positive stress test, and/or previous coronary revascularization or myocardial infarction) compared with healthy subjects in small studies.^{129,130} However, limited reporting of CVD risk factors, the inclusion patients with diabetes, and a high CVD risk control group weaken these associations.^{129,130} A recent study using spectral domain OCT examined a subgroup of 764 elderly patients (mean age 82 years; two-thirds female patients) from a French population-based study (>9000 participants) and found no associations between subfoveal choroidal thickness and previous CVD, current CVD risk factors, or estimated future CVD risk according to a clinical scoring tool.¹³¹ A large amount of missing data, recall bias from patient-declared medical history, and a single manual measure of choroidal thickness may have contributed to these negative results.

There are no data linking OCT metrics to incident CVD to extend the relevance of the associations presented. These data are likely to appear soon, and whether OCT-derived metrics can outperform photography-derived metrics in predicting CKD and CVD outcomes is an important test of their potential utility. An additional area that warrants exploration is the extent to which retinal OCT metrics are modifiable by interventions such as lowering BP, reducing proteinuria, or restoring kidney function. Such data might allow OCT-derived metrics to be developed from biomarkers into easily assessable surrogate end points for clinical trials.

Figure 4 | (continued) as the area bounded by the internal limiting membrane (ILM) and Bruch's membrane (BM). **(b)** Left panel: a CLSO image centered over the optic nerve head, with the line of the cross section (green) circled around the peripapillary region. The dark blue line defines the distance from the optic disc to the fovea. Right panel: an OCT image demonstrating retinal thickness from the circular cross section around the optic nerve head in the left image. The green line running from left to right corresponds to the direction of the cross section of the green circle in the left panel. *Retinal nerve fiber layer* (RNFL) thickness is defined as the area bordered by red and cyan lines. **(c)** CSLO (left panel) and OCT with enhanced depth imaging (EDI) (right panel) in a healthy subject. EDI enables the identification of deeper structures, including the highly vascularized choroid. We measured choroidal thickness at 3 locations: I = 2 mm nasal to the fovea, II = subfoveal, and III = 2 mm temporal to the fovea. The corresponding locations on the macula are indicated by yellow arrows. **(d)** CLSO (left panel) and OCT with EDI (right panel) in an age- and sex-matched subject with CKD demonstrating comparative thinning of the choroid at all 3 locations. The corresponding locations on the macula are indicated by yellow arrows. To optimize viewing of this image, please see the online version of this article at www.kidney-international.org.

Table 4 | Hemodialysis and OCT metrics^a

Study	Year	Country	Device	N	Age (yr)	Proportion with diabetes (%)	Dialysis vintage (yr)	Achieved UF		ΔWeight	ΔBP	ΔIOP	ΔRetinal thickness	ΔChoroidal thickness	ΔRNFL	ΔVessel density
								Volume (L)								
Shin <i>et al.</i> ¹¹³	2019	South Korea	DRI Triton (Topcon, Tokyo, Japan)	32	56	~66	6	3	↓2.6 kg	↓SBP ~12 mm Hg	No change	-	↓~5%	-	-	
Shin <i>et al.</i> ¹¹⁴	2018	South Korea	DRI OCT1 (Topcon Atlantis)	29	56	~52	5.8	3	↓2.7 kg	↓SBP ~10 mm Hg	No change	No change	↓~7%	-	↓~3%	
Zhang <i>et al.</i> ¹¹⁵	2018	China	AngioVue (OptoVue, CA)	77	53	~50	4.5	2.5	-	↓SBP ~7 mm Hg	No change	↓~2%	No change	-	↓~3%	
Chen <i>et al.</i> ¹¹⁶	2018	China	Cirrus HD (Carl Zeiss AG, Jena, Germany)	90	58	~13	5.8	-	-	↓SBP ~10 mm Hg	No change	No change	↓~12%	↑~3%	-	
Chang <i>et al.</i> ¹¹⁷	2017	South Korea	SPECTRALIS with EDI (Heidelberg Engineering, Heidelberg, Germany)	54	60	~60	5	-	↓2.3 kg	↓SBP ~15 mm Hg	↓~10%	-	↓~10%	No change	-	
Ishibazawa <i>et al.</i> ¹¹⁸	2015	Japan	RetinaScan (Nidek, Gamagori, Japan) No EDI	77	67	~50	4.7	2.5	↓2.2 kg	↓SBP ~14 mm Hg	No change	No change	↓~10%	-	-	
Jung <i>et al.</i> ¹¹⁹	2014	South Korea	SPECTRALIS (Heidelberg Engineering) No EDI	19	51	~50	3.5	-	↓2.1 kg	↓SBP ~16 mm Hg	No change	-	↑~5%	-	-	
Yang <i>et al.</i> ¹²⁰	2013	South Korea	SPECTRALIS with EDI (Heidelberg Engineering)	34	58	~25	6	-	↓2.8 kg	No change	↓~10%	No change	↓~6%	No change	-	
Ulas <i>et al.</i> ¹²¹	2013	Turkey	SPECTRALIS with EDI (Heidelberg Engineering)	21	61	-	2.4	3	-	No change	No change	No change	↓~10%	-	-	
Jung <i>et al.</i> ¹²²	2013	South Korea	SPECTRALIS No EDI (Heidelberg Engineering)	30	54	~40	4.3	-	↓1.9 kg	↓SBP ~17 mm Hg	↓~15%	↓~2%	-	-	-	
Theodossiadis <i>et al.</i> ¹²³	2012	Greece	OCT3 Stratus (Carl Zeiss AG)	72	62	100	2.8	-	↓2.5 kg	No change	-	↓~4%	-	-	-	
Demir <i>et al.</i> ¹²⁴	2009	Turkey	OCT3 Stratus (Carl Zeiss AG)	36	41	-	3.5	-	-	-	-	-	-	No change	-	

↑, increase; ↓, decrease; BP, blood pressure; DBP, diastolic blood pressure; EDI, enhanced depth imaging; IOP, intraocular pressure; OCT, optical coherence tomography; RNFL, retinal nerve fiber layer; SBP, systolic blood pressure; UF, ultrafiltration.

^aStudies examining OCT metrics before and after a hemodialysis session in patients on long-term renal replacement therapy.

All values are mean.

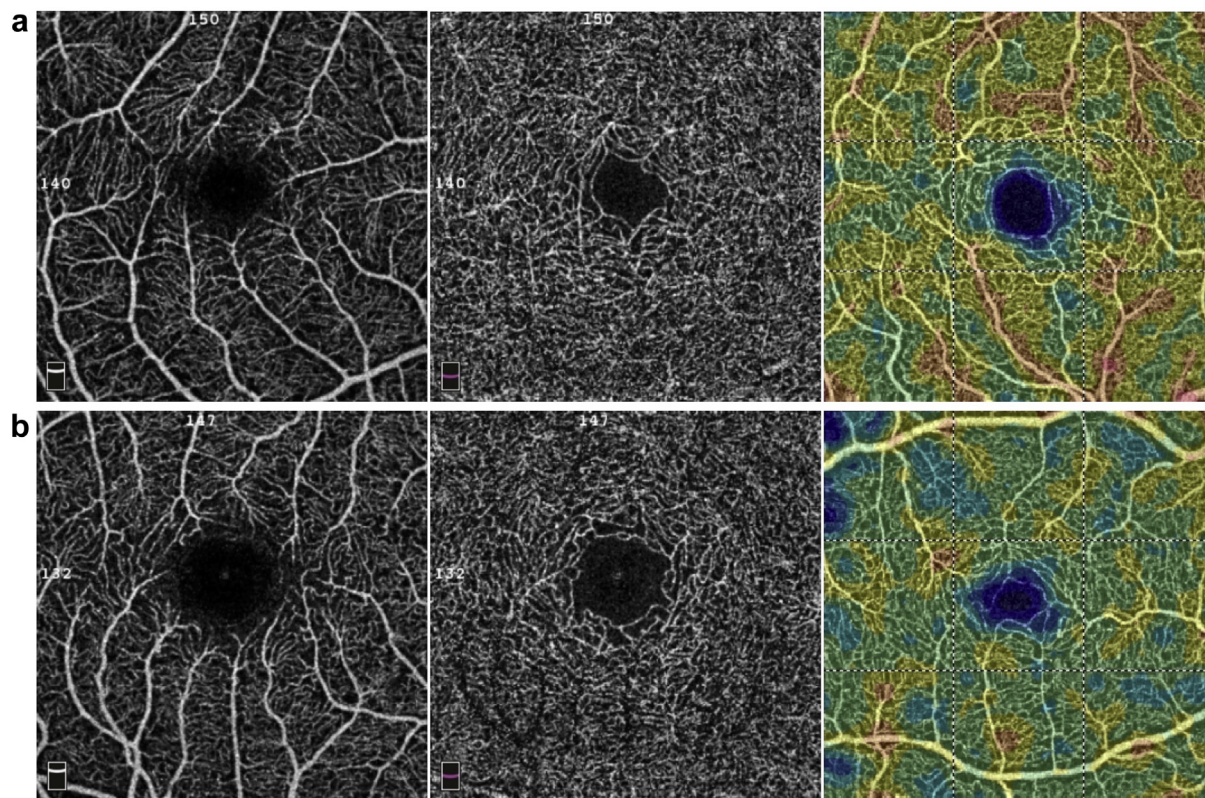


Figure 5 | Optical coherence tomography (OCT) angiography in health and chronic kidney disease (CKD). *En face* OCT angiograms of the right eye centered on the macula taken using the AngioVue Imaging System (Optovue, Inc., Fremont, CA) in (a) a healthy volunteer and (b) an age- and sex-matched patient with proteinuric CKD. Left and middle panels: perimacular superficial and deep capillary plexuses with the foveal avascular zone (FAZ) represented by the central black circular region. Compared with a healthy volunteer, a wider FAZ and a disorganized branching pattern are evident in the patient with CKD and are suggestive of rarefaction and microvascular damage. Right panels: perimacular superficial retinal vessels and the FAZ with color map overlays of software-calculated vessel density. Red denotes high vessel density; green denotes moderate vessel density; and blue/navy denotes low vessel density. There are fewer regions with high/moderate vessel density (red/green regions) in the patient with CKD than in the healthy volunteer. Note that these images are not from the same subjects as the images in the left and middle panels. To optimize viewing of this image, please see the online version of this article at www.kidney-international.org.

OCT angiography

Retinal OCT angiography (OCT-A) combines structural and functional imaging by analyzing the changing variance in light speckle created by erythrocyte flow over multiple scans. This generates a contrast-free angiogram down to the capillary level and surrogate indices of perfusion (Figure 5).⁸⁹ Most OCT-A platforms have integrated software that automatically segments the OCT images alongside angiographic data to report global and regional vessel density for each retinal layer (Supplementary Figure S5 and Supplementary Movies S3 and S4). OCT-A images can also be used to assess *Df* and the geometry of the foveal avascular zone, with widening indicative of capillary dropout (Figure 5). Visualization of these terminal branches of the vascular tree may allow earlier, more precise detection of local and systemic microvascular disease. Small clinical studies of age-related macular degeneration¹³² and diabetic retinopathy¹³³ have used OCT-A to demonstrate novel structural vessel pathology with an apparent reduction in perfusion. Limitations of OCT-A include a susceptibility to movement artifact degradation and a lack of

true perfusion indices. Doppler OCT, which detects the frequency shift of backscattered light from erythrocytes, allowing determination of blood flow velocity alongside vessel dimensions, may overcome the latter issue.⁸⁹

Hypertension, diabetes mellitus, and CKD. Data supporting a potential role of OCT-A in systemic diseases are emerging. A study of Asian patients with hypertension found that those with poor BP control (assessed by 24-hour ambulatory monitoring) had a lower deep capillary plexus vessel density than did those with optimal BP control.¹¹⁰ These groups were well matched in terms of age, sex, CVD risk factors, and renal function (mean eGFR ~ 90 ml/min per 1.73 m²), but the poorly controlled group had higher microalbuminuria.¹¹⁰ In adjusted analyses, suboptimal BP control, increasing BP, and worsening eGFR were associated with worse capillary rarefaction.¹¹⁰ An Italian study extended these findings by using OCT-A in 120 hypertensive patients with and without CKD to report a lower vessel density in both superficial and deep capillary plexuses in those with CKD.¹³⁴ The inclusion of patients with more severe renal impairment and higher

proteinuria in this study¹³⁴ may explain the more extensive retinal vessel rarefaction seen as compared with the Singapore study.¹¹⁰ However, it is important to note that different OCT-A devices were used by each center.

In diabetes, larger foveal avascular zone area, lower retinal capillary density, and reduced *Df* have been shown to predict progression of diabetic retinopathy.¹³⁵ A recent study using OCT-A has suggested a potential vascular basis for GCL thinning in diabetes.¹³⁶ Patients with no detectable retinopathy, with a short duration of diabetes (~8 years) and normal renal function, had significant GCL thinning that was independently associated with lower retinal capillary density and perfusion, suggesting a structural or functional vascular origin.¹³⁶ This hypothesis is countered by preclinical and clinical data, suggesting that GCL thinning can occur without alterations in histologically assessed capillary density.¹³⁷ In summary, GCL thinning appears early in diabetes, potentially before structural vascular changes but convincingly before overt target organ damage. The earliest functional changes in the diabetic kidney are glomerular hyperfiltration and hypertension,¹³⁸ and detecting this would be useful in guiding intervention and treatment efficacy. Whether GCL thinning or changes in GCL perfusion can act as an early marker of tissue dysfunction in diabetes such as glomerular hyperfiltration and hypertension warrants further detailed study. There are few data in diabetic CKD, but a recent study using OCT-A in 184 patients with type 2 diabetes suggested that a reduced retinal capillary density independently predicted coexisting CKD and its severity.¹³⁹

Given the association with risk factors for CKD progression, data linking OCT-A to long-term renal outcomes should soon emerge. However, identifying patients at risk of acute kidney injury (AKI) is also important as AKI confers an increased risk of future CKD¹⁴⁰ and CVD.¹⁴¹ OCT-A–derived retinal vessel density was recently shown to predict the risk of contrast-induced AKI after angiography for acute coronary syndrome.¹⁴² Moreover, the addition of OCT-A metrics to the current contrast-induced AKI risk assessment tools improved prediction of AKI by ~10%.¹⁴²

CVD outcomes. As with OCT, data linking OCT-A metrics to incident CVD are lacking. With respect to prevalent CVD, a study of 246 patients presenting with acute coronary syndrome found that these patients had reduced inner retinal vessel density as compared with a limited number of age- and sex-matched controls.¹⁴³ In addition, more severe rarefaction correlated with a higher CVD risk as defined by the American Heart Association and Global Registry of Acute Coronary Events scoring systems.¹⁴³

Dynamic functional imaging

Laser Doppler flowmetry and flicker response imaging can assess retinal vascular endothelial function in a dynamic manner. Studies examining laser flicker–induced vascular responses have shown impaired retinal endothelium–dependent vasodilatation in patients with CVD risk factors

including albuminuria,¹⁴⁴ prediabetes,¹⁴⁵ early hypertension,¹⁴⁶ preeclampsia,¹⁴⁷ and hypercholesterolemia.¹⁴⁸ In addition, a recent study reported worsening retinal endothelial function (as measured by the degree of laser flicker–induced vasodilatation) between healthy subjects, those at risk of CVD, and those with overt CVD,¹⁴⁹ supporting the potential to stratify patients. Limitations of these techniques include the need for mydriasis, longer acquisition time compared to other imaging techniques, and assessment of retinal vessels alone.

VISIONS FOR THE FUTURE

Preclinical OCT

Preclinical OCT allows simultaneous noninvasive longitudinal imaging of the eye in disease models and may provide novel insights into the underlying mechanisms. We have used OCT to explore the links between the eye and the kidney and shown that mice with hypertension alone had no choroidal thinning whereas mice with matched hypertension but with coexisting renal injury developed significant thinning.⁹⁶ This technology is being refined but has been used to perform detailed structural, functional, and biochemical assessments in various models of retinopathy.¹⁵⁰

Big data

The recognition of the potential power of OCT beyond eye disease is evidenced by its inclusion in the UK Biobank study between 2006 and 2010.¹⁵¹ The UK Biobank obtained OCT images from >67,000 participants (of whom >35,000 were healthy) along with sociodemographic, cognitive, CVD, and renal risk measures. This could provide novel robust epidemiological data to establish healthy ranges and generate evidence of OCT metrics as prognostic disease biomarkers. The expansion of OCT out-of-hospital settings and into the community is already in progress, with the leading optometry chain in the United Kingdom announcing a rollout of OCT devices across all outlets.¹⁵²

Deep learning

Machine learning involves programming computers to detect patterns in raw data on the basis of explicit parameters set by the operator. Such techniques have been used to automate the classification of diabetic retinopathy from fundus photographs but can be intensive to engineer and supervise. Deep learning is an extension of machine learning whereby predictive patterns are learned and refined by the machine itself by using an algorithm developed from a large example data set such as a bank of graded retinal images.¹⁵³ Multiple levels of increasingly abstract pattern recognition enable the algorithm to develop complex neural networks that are highly accurate, require minimal engineering, and can match expert human performance as shown recently with diabetic retinopathy.¹⁵⁴

Recent work in this field has used retinal photographs and clinical data from >280,000 patients to train an algorithm to predict a range of CVD risk factors from 2 separate banks of

retinal photographs totaling ~13,000 patients.¹⁵⁵ The algorithm displayed impressive accuracy: sex (area under the curve, 0.97), smoking status (area under the curve 0.71), age (mean absolute error ~3 years), and systolic BP (mean absolute error ~11 mm Hg).¹⁵⁵ For predicting incident CVD risk, the algorithm offered little improvement over a conventional CVD risk scoring tool but encouragingly showed similar power. More recently, one of the authors of this review (PAK) coled the development of a deep learning algorithm that allows triage and diagnosis of the commonest sight-threatening retinal diseases from OCT scans.¹⁵⁶ When applied to a large retrospective data set, this algorithm demonstrated diagnostic accuracy equivalent to that of specialist ophthalmologists. Prospective clinical trials of this algorithm are now planned. Importantly, the algorithm also creates an intermediate representation of the retinal anatomy/pathology and thus addresses, in part, the concerns raised by clinicians regarding artificial intelligence systems that can be often perceived as *black boxes* dictating clinical care. This approach will likely be readily transferable from ophthalmic to systemic disease, offering novel insights and generating new hypotheses.

Challenges

The real-world utility of the retinal vascular metrics for CVD risk profiling over currently available tools is uncertain. Well-designed studies show that such metrics can offer a small benefit (~10%) over current tools in identifying high-risk patients.^{65,80,88} Whether this is sufficient for integration into clinical practice is not known, nor is how best to act on them. The high fidelity and granular nature of OCT data may yield novel metrics that extend risk stratification beyond what retinal photography has achieved. Preclinical and clinical studies with longitudinal imaging and data linkage, currently available in only a few countries, will be required to confirm this. However, the highly competitive commercial interest in retinal OCT has led to the emergence of several devices each with unique retinal layer segmentation algorithms and so metrics are not interchangeable across devices.^{157,158} Finally, maximizing the yield of data from complex OCT and OCT-A images will require similar advancement and investment in imaging analysis methodology, which, given the advent of artificial intelligence in health care, is an exciting field in itself.

CONCLUSIONS

The eye offers a well-defined target organ whose microvessel network is homologous to that in kidney in both health and disease. The chorioretinal microvasculature can now be precisely mapped, measured, and tracked. Quantitative vessel analysis of retinal photographs has provided a strong rationale for the eye to report and stratify CVD risk, but this is yet to transition into clinical practice. Novel modalities such as OCT have undergone rapid clinical expansion and have shown potential in detecting microvascular changes that are associated with surrogate markers of increased renal and CVD risk. Advances in data analysis and machine learning may soon

enable clinicians to generate individualized chorioretinal risk scores to identify patients at risk of adverse outcomes on the basis of precise segmented OCT metrics. The advancement of multimodal functional retinal imaging has brought the previously distant goal of noninvasive functional microvascular assessment into sharp focus and the near-term.

DISCLOSURE

All the authors declared no competing interests.

ACKNOWLEDGMENTS

TEF was supported by a Medical Research Council Clinical Research Training Fellowship. PAK was supported by an NIHR Clinician Scientist Fellowship. ND was supported by a British Heart Foundation Intermediate Clinical Research Fellowship.

SUPPLEMENTARY MATERIAL

[Supplementary File \(PDF\)](#)

Table S1. Retinal vascular metrics to predict incident hypertension.

Table S2. Retinal vascular metrics to predict incident diabetes mellitus.

Table S3. Retinal vascular metrics to predict cardiovascular disease.

Figure S1. Alport syndrome-associated retinopathy. Ultrawide field scanning laser ophthalmoscope photograph of the left eye of a male patient with end-stage renal disease secondary to X-linked Alport syndrome. The characteristic dot-and-fleck retinopathy is evident as green perimacular deposits in the center of the image. There is also associated loss of the foveal reflex due to macular thinning. The presence of Alport syndrome-associated retinopathy can help diagnosis, suggest inheritance patterns, identify those at risk of progressive chronic kidney disease, and differentiate from mimics such as thin glomerular basement membrane disease that has no associated retinal features.^{14,15}

Figure S2. Retinal photography and fundus retinal caliber assessment. (A) Digital retinal photograph of the right eye taken using the Canon CR-1 fundus camera with a field of view of 45°. (B) Scanning laser ophthalmoscope image of the right eye centered over the optic disc taken using the SPECTRALIS spectral domain optical coherence tomography machine (SD-OCT; Heidelberg Engineering, Heidelberg, Germany). The center of the optic disc is manually determined. A standard set of concentric circular measurement zones commonly used in the analysis of fundus camera images is mapped from this point as shown. Zone A is the area 0.5 to 1 optic disc diameters away from the center as bounded by the white dotted lines. The vessel analysis software VAMPIRE (University of Dundee, Dundee, UK) selects the 6 widest arterioles (red) and venules (blue) crossing zone A to calculate central retinal arteriolar equivalent, central retinal venular equivalent, and arteriole-to-venule ratio.

Figure S3. Retinal optical coherence tomography. Blue lines represent fiber paths; red lines represent optical paths; And green lines represent signal paths. Low coherence light (typically ~800 nm wavelength) is split into a sample beam and a reference beam. The sample beam is shone onto the retina and reflected back as *light echoes*. The reference beam is directed to a mirror positioned at a known distance from the light source. A range of *sample* light echoes each return at different times depending on the distance of the reflecting tissue from the light source. Returning *sample* and *reference* light echoes are reunited and directed to a photodetector. An interference signal is detected when the time delays between the sample and reference light echoes is small; that is, the distance of the reference mirror matches the distance of the reflecting tissue. Moving

the reference mirror (positions A–C) alters the distance the reference beam/echo must travel and thus changes the time delay between the reference and sample echoes. At each new reference mirror distance, the reference echo time delay will closely match a different sample echo time delay, generating a new interference signal corresponding to a deeper/shallower reflecting tissue layer. A sequential movement of the reference mirror allows the construction of a single interference depth profile: the A scan. A scans obtain depth profiles along the z axis. The lateral scanning mirror is rotated through positions 1 to 4 along the x axis to obtain sequential adjacent A scans, which are used to generate a single horizontal B scan. The vertical scanning mirror is elevated/lowered along the y axis to obtain horizontal B scans at multiple levels. B scans can then be stacked to create a volume scan (Supplementary Movies S1 and S2).

Figure S4. Retinal layer segmentation by optical coherence tomography (OCT). Close-up of the horizontal line OCT scan through the macula of the right eye with an automated segmentation of individual retinal layers. BM, Bruch's membrane; CH, choroid; GCL, ganglion cell layer; INL, inner nuclear layer; IPL, inner plexiform layer; ONL, outer nuclear layer; OPL, outer plexiform layer; PR, photoreceptor layer; RNFL, retinal nerve fiber layer; RPE, retinal pigment epithelium.

Figure S5. Optical coherence tomography (OCT) angiography. 3×3 mm OCT angiograms *en face* (left panels) and in cross section (right panels) of the right eye centered on the macula taken using the AngioVue Imaging System (Optovue, Inc., Fremont, CA). **(A)** Left panel: the perimacular superficial capillary plexus and the foveal avascular zone. Right panel: the OCT image showing the level and boundaries of inner (superficial) retinal layer segmentation that corresponds to the *en face* angiogram. Red and green lines define the upper and lower limits of the segmentation band, respectively. **(B)** Left panel: the perimacular deep capillary plexus and the foveal avascular zone. Right panel: the OCT image showing the level and boundaries of deeper retinal layer segmentation that corresponds to the *en face* angiogram. Red and green lines define the upper and lower limits of the segmentation band, respectively. **(C)** Left panel: The outer (deepest) retinal layers are relatively avascular as shown and is thus dependent on passive oxygenation from the deeper choroidal circulation. Right panel: the OCT image showing the level and boundaries of outer retinal layer segmentation that corresponds to the *en face* angiogram. Red lines define the upper and lower limits of the segmentation band. **(D)** Left panel: The subfoveal choriocapillaris is a dense mesh of capillaries underneath the pigment epithelium. Despite advances in OCT angiography, imaging discrete vessels here remains challenging. Right panel: the OCT image showing the level and boundaries of choriocapillaris segmentation that corresponds to the *en face* angiogram. Red and green lines define the upper and lower limits of the segmentation band, respectively.

Movie S1. Optical coherence tomography (OCT) in health. Movie of a 3-dimensional rendered macular volume OCT scan of the right eye of a healthy volunteer.

Movie S2. Optical coherence tomography (OCT) in chronic kidney disease (CKD). Movie of a 3-dimensional rendered macular volume OCT scan of the right eye of an age- and sex-matched subject with CKD. Note the marked thinning of choroidal vascular layer lying underneath the retina.

Movie S3. Optical coherence tomography (OCT) angiography of the macula in health. Movie of the sequential *layer-by-layer* OCT angiograms centered on the macula of the right eye of a healthy volunteer. The track bar on the left-hand side relates the color-coded anatomical localization of retinal regions that correspond to the angiograms shown in the main panel.

Movie S4. Optical coherence tomography (OCT) angiography of the optic disc in health. Movie of the sequential *layer-by-layer* OCT angiograms centered on the fundus of the right eye of a healthy volunteer. The track bar on the left-hand side relates the color-coded anatomical localization of retinal regions that correspond to the angiograms shown in the main panel.

REFERENCES

- Gansevoort RT, Correa-Rotter R, Hemmelgarn BR, et al. Chronic kidney disease and cardiovascular risk: epidemiology, mechanisms, and prevention. *Lancet*. 2013;382:339–352.
- Kearney PM, Whelton M, Reynolds K, et al. Global burden of hypertension: analysis of worldwide data. *Lancet*. 2005;365:217–223.
- Sarwar N, Gao P, Seshasai SR, et al. Diabetes mellitus, fasting blood glucose concentration, and risk of vascular disease: a collaborative meta-analysis of 102 prospective studies. *Lancet*. 2010;375:2215–2222.
- Thomas B, Matsushita K, Abate KH, et al. Global cardiovascular and renal outcomes of reduced GFR. *J Am Soc Nephrol*. 2017;28:2167–2179.
- Brunner H, Cockcroft JR, Deanfield J, et al. Endothelial function and dysfunction. Part II: Association with cardiovascular risk factors and diseases. A statement by the Working Group on Endothelins and Endothelial Factors of the European Society of Hypertension. *J Hypertens*. 2005;23:233–246.
- Houben A, Martens RJH, Stehouwer CDA. Assessing microvascular function in humans from a chronic disease perspective. *J Am Soc Nephrol*. 2017;28:3461–3472.
- Stehouwer CDA. Microvascular dysfunction and hyperglycemia: a vicious cycle with widespread consequences. *Diabetes*. 2018;67:1729–1741.
- Halcox JP, Schenke WH, Zalos G, et al. Prognostic value of coronary vascular endothelial dysfunction. *Circulation*. 2002;106:653–658.
- Remuzzi A, Sangalli F, Macconi D, et al. Regression of renal disease by angiotensin II antagonism is caused by regeneration of kidney vasculature. *J Am Soc Nephrol*. 2016;27:699–705.
- Anderson TJ, Uehata A, Gerhard MD, et al. Close relation of endothelial function in the human coronary and peripheral circulations. *J Am Coll Cardiol*. 1995;26:1235–1241.
- Bonetti PO, Pumper GM, Higano ST, et al. Noninvasive identification of patients with early coronary atherosclerosis by assessment of digital reactive hyperemia. *J Am Coll Cardiol*. 2004;44:2137–2141.
- Booij JC, Baas DC, Beisekeeva J, et al. The dynamic nature of Bruch's membrane. *Prog Retin Eye Res*. 2010;29:1–18.
- Boutaud A, Borza D-B, Bondar O, et al. Type IV collagen of the glomerular basement membrane. *J Biol Chem*. 2000;275:30716–30724.
- Savige J, Sheth S, Leys A, et al. Ocular features in Alport's syndrome: pathogenesis and clinical significance. *Clin J Am Soc Nephrol*. 2015;10:703–709.
- Colville D, Savage J, Branley P, Wilson D. Ocular abnormalities in thin basement membrane disease. *Br J Ophthalmol*. 1997;81:373–377.
- McAdoo SP, Pusey CD. Anti-glomerular basement membrane disease. *Clin J Am Soc Nephrol*. 2017;12:1162–1172.
- Jampol LM, Lahov M, Albert DM, Craft J. Ocular clinical findings and basement membrane changes in Goodpasture's syndrome. *Am J Ophthalmol*. 1975;79:452–463.
- Rowe PA, Mansfield DC, Dutton GN. Ophthalmic features of fourteen cases of Goodpasture's syndrome. *Nephron*. 1994;68:52–56.
- McAvoy CE, Silvestri G. Retinal changes associated with type 2 glomerulonephritis. *Eye*. 2005;19:985–989.
- Sethi S, Fervenza FC. Membranoproliferative glomerulonephritis—a new look at an old entity. *N Engl J Med*. 2012;366:1119–1131.
- Whitmore SS, Sohn EH, Chirco KR, et al. Complement activation and choriocapillaris loss in early AMD: implications for pathophysiology and therapy. *Prog Retin Eye Res*. 2015;45:1–29.
- Dalvin LA, Fervenza FC, Sethi S, Pulido JS. Manifestations of complement-mediated and immune complex-mediated membranoproliferative glomerulonephritis: a comparative consecutive series. *Ophthalmology*. 2016;123:1588–1594.
- Hughes S, Yang H, Chan-Ling T. Vascularization of the human fetal retina: roles of vasculogenesis and angiogenesis. *Invest Ophthalmol Vis Sci*. 2000;41:1217–1228.

24. Sequeira Lopez ML, Gomez RA. Development of the renal arterioles. *J Am Soc Nephrol*. 2011;22:2156–2165.
25. Nickla DL, Wallman J. The multifunctional choroid. *Prog Retin Eye Res*. 2010;29:144–168.
26. Munro DAD, Davies JA. Vascularizing the kidney in the embryo and organoid: questioning assumptions about renal vasculogenesis. *J Am Soc Nephrol*. 2018;29:1593–1595.
27. Anand-Apte B, Hollyfield JG. Developmental anatomy of the retinal and choroidal vasculature. In: Dratt D, Besharse J, Dana R, eds. *Encyclopedia of the Eye*. Amsterdam: Elsevier; 2010:9–15.
28. Haraldsson B, Nystrom J, Deen WM. Properties of the glomerular barrier and mechanisms of proteinuria. *Physiol Rev*. 2008;88:451–487.
29. Wilkinson-Berka JL, Agrotis A, Deliyanti D. The retinal renin-angiotensin system: roles of angiotensin II and aldosterone. *Peptides*. 2012;36:142–150.
30. Rockwood EJ, Fantes F, Davis EB, Anderson DR. The response of retinal vasculature to angiotensin. *Invest Ophthalmol Vis Sci*. 1987;28:676–682.
31. Fletcher EL, Phipps JA, Ward MM, et al. The renin-angiotensin system in retinal health and disease: its influence on neurons, glia and the vasculature. *Prog Retin Eye Res*. 2010;29:284–311.
32. Mauer M, Zinman B, Gardiner R, et al. Renal and retinal effects of enalapril and losartan in type 1 diabetes. *N Engl J Med*. 2009;361:40–51.
33. MacCumber MW, D'Anna SA. Endothelin receptor-binding subtypes in the human retina and choroid. *Arch Ophthalmol*. 1994;112:1231–1235.
34. Chou JC, Rollins SD, Ye M, et al. Endothelin receptor-A antagonist attenuates retinal vascular and neuroretinal pathology in diabetic mice. *Invest Ophthalmol Vis Sci*. 2014;55:2516–2525.
35. Dhaun N, Goddard J, Webb DJ. The endothelin system and its antagonism in chronic kidney disease. *J Am Soc Nephrol*. 2006;17:943–955.
36. Heerspink HJL, Parving H-H, Andress DL, et al. Atrasentan and renal events in patients with type 2 diabetes and chronic kidney disease (SONAR): a double-blind, randomised, placebo-controlled trial. *Lancet*. 2019;393:1937–1947.
37. Wong TY, Mitchell P. The eye in hypertension. *Lancet*. 2007;369:425–435.
38. Murray CD. The physiological principle of minimum work: I. The vascular system and the cost of blood volume. *Proc Natl Acad Sci U S A*. 1926;12:207–214.
39. Patton N, Aslam TM, MacGillivray T, et al. Retinal image analysis: concepts, applications and potential. *Prog Retin Eye Res*. 2006;25:99–127.
40. Cheung CY, Ikram MK, Sabanayagam C, Wong TY. Retinal microvasculature as a model to study the manifestations of hypertension. *Hypertension*. 2012;60:1094–1103.
41. Wei FF, Zhang ZY, Thijs L, et al. Conventional and ambulatory blood pressure as predictors of retinal arteriolar narrowing. *Hypertension*. 2016;68:511–520.
42. Liew G, Wang JJ, Cheung N, et al. The retinal vasculature as a fractal: methodology, reliability, and relationship to blood pressure. *Ophthalmology*. 2008;115:1951–1956.
43. Cheung CY, Tay WT, Mitchell P, et al. Quantitative and qualitative retinal microvascular characteristics and blood pressure. *J Hypertens*. 2011;29:1380–1391.
44. Cheung CY, Thomas GN, Tay W, et al. Retinal vascular fractal dimension and its relationship with cardiovascular and ocular risk factors. *Am J Ophthalmol*. 2012;154:663–674.e661.
45. Kurniawan ED, Cheung N, Cheung CY, et al. Elevated blood pressure is associated with rarefaction of the retinal vasculature in children. *Invest Ophthalmol Vis Sci*. 2012;53:470–474.
46. Nguyen TT, Wang JJ, Sharrett AR, et al. Relationship of retinal vascular caliber with diabetes and retinopathy: the Multi-Ethnic Study of Atherosclerosis (MESA). *Diabetes Care*. 2008;31:544–549.
47. Saldívar E, Cabrales P, Tsai AG, Intaglietta M. Microcirculatory changes during chronic adaptation to hypoxia. *Am J Physiol Heart Circ Physiol*. 2003;285:H2064–H2071.
48. Nguyen TT, Islam FM, Farouque HM, et al. Retinal vascular caliber and brachial flow-mediated dilation: the Multi-Ethnic Study of Atherosclerosis. *Stroke*. 2010;41:1343–1348.
49. Ikram MK, de Jong FJ, Vingerling JR, et al. Are retinal arteriolar or venular diameters associated with markers for cardiovascular disorders? The Rotterdam Study. *Invest Ophthalmol Vis Sci*. 2004;45:2129–2134.
50. Klein R, Klein BEK, Moss SE, et al. Retinal vascular abnormalities in persons with type 1 diabetes: the Wisconsin Epidemiologic Study of Diabetic Retinopathy: XVIII. *Ophthalmology*. 2003;110:2118–2125.
51. Klein R, Klein BEK, Moss SE, et al. Retinal vascular caliber in persons with type 2 diabetes: the Wisconsin Epidemiological Study of Diabetic Retinopathy: XX. *Ophthalmology*. 2006;113:1488–1498.
52. Owen CG, Rudnicka AR, Welikala RA, et al. Retinal vasculometry associations with cardiometabolic risk factors in the European Prospective Investigation of Cancer-Norfolk Study. *Ophthalmology*. 2019;126:96–106.
53. Sabanayagam C, Lye WK, Klein R, et al. Retinal microvascular calibre and risk of diabetes mellitus: a systematic review and participant-level meta-analysis. *Diabetologia*. 2015;58:2476–2485.
54. Grauslund J, Green A, Kawasaki R, et al. Retinal vascular fractals and microvascular and macrovascular complications in type 1 diabetes. *Ophthalmology*. 2010;117:1400–1405.
55. Cheung CY, Sabanayagam C, Law AK, et al. Retinal vascular geometry and 6 year incidence and progression of diabetic retinopathy. *Diabetologia*. 2017;60:1770–1781.
56. Grunwald JE, Alexander J, Maguire M, et al. Prevalence of ocular fundus pathology in patients with chronic kidney disease. *Clin J Am Soc Nephrol*. 2010;5:867–873.
57. Grunwald JE, Alexander J, Ying GS, et al. Retinopathy and chronic kidney disease in the Chronic Renal Insufficiency Cohort (CRIC) study. *Arch Ophthalmol*. 2012;130:1136–1144.
58. Wong TY, Coresh J, Klein R, et al. Retinal microvascular abnormalities and renal dysfunction: the Atherosclerosis Risk in Communities Study. *J Am Soc Nephrol*. 2004;15:2469–2476.
59. Grunwald JE, Pistilli M, Ying G-S, et al. Association between progression of retinopathy and concurrent progression of kidney disease: findings from the Chronic Renal Insufficiency Cohort (CRIC) study. *JAMA Ophthalmol*. 2019;137:767–774.
60. Wong CW, Wong TY, Cheng CY, Sabanayagam C. Kidney and eye diseases: common risk factors, etiological mechanisms, and pathways. *Kidney Int*. 2014;85:1290–1302.
61. Wong TY, Shankar A, Klein R, Klein BE. Retinal vessel diameters and the incidence of gross proteinuria and renal insufficiency in people with type 1 diabetes. *Diabetes*. 2004;53:179–184.
62. Edwards MS, Wilson DB, Craven TE, et al. Associations between retinal microvascular abnormalities and declining renal function in the elderly population: the Cardiovascular Health Study. *Am J Kidney Dis*. 2005;46:214–224.
63. Sabanayagam C, Shankar A, Klein BE, et al. Bidirectional association of retinal vessel diameters and estimated GFR decline: the Beaver Dam CKD Study. *Am J Kidney Dis*. 2011;57:682–691.
64. Yau JW, Xie J, Kawasaki R, et al. Retinal arteriolar narrowing and subsequent development of CKD stage 3: the Multi-Ethnic Study of Atherosclerosis (MESA). *Am J Kidney Dis*. 2011;58:39–46.
65. Baumann M, Burkhardt K, Heemann U. Microcirculatory marker for the prediction of renal end points: a prospective cohort study in patients with chronic kidney disease stage 2 to 4. *Hypertension*. 2014;64:338–346.
66. Grunwald JE, Pistilli M, Ying GS, et al. Retinopathy and progression of CKD: the CRIC study. *Clin J Am Soc Nephrol*. 2014;9:1217–1224.
67. Yip W, Sabanayagam C, Teo BW, et al. Retinal microvascular abnormalities and risk of renal failure in Asian populations. *PLoS One*. 2015;10:e0118076.
68. Yip W, Ong PG, Teo BW, et al. Retinal vascular imaging markers and incident chronic kidney disease: a prospective cohort study. *Sci Rep*. 2017;7:9374.
69. McKay GJ, Paterson EN, Maxwell AP, et al. Retinal microvascular parameters are not associated with reduced renal function in a study of individuals with type 2 diabetes. *Sci Rep*. 2018;8:3931.
70. Awua-Larbi S, Wong TY, Cotch MF, et al. Retinal arteriolar caliber and urine albumin excretion: the Multi-Ethnic Study of Atherosclerosis. *Nephrol Dial Transplant*. 2011;26:3523–3528.
71. Klein R, Knudtson MD, Klein BE, et al. The relationship of retinal vessel diameter to changes in diabetic nephropathy structural variables in patients with type 1 diabetes. *Diabetologia*. 2010;53:1638–1646.
72. Sng CC, Sabanayagam C, Lamoureux EL, et al. Fractal analysis of the retinal vasculature and chronic kidney disease. *Nephrol Dial Transplant*. 2010;25:2252–2258.

73. Lim LS, Cheung CY, Sabanayagam C, et al. Structural changes in the retinal microvasculature and renal function. *Invest Ophthalmol Vis Sci.* 2013;54:2970–2976.
74. McGowan A, Silvestri G, Moore E, et al. Evaluation of the retinal vasculature in hypertension and chronic kidney disease in an elderly population of Irish nuns. *PLoS One.* 2015;10:e0136434.
75. Wong TY, Klein R, Sharrett AR, et al. The prevalence and risk factors of retinal microvascular abnormalities in older persons: the Cardiovascular Health Study. *Ophthalmology.* 2003;110:658–666.
76. Cooper LS, Wong TY, Klein R, et al. Retinal microvascular abnormalities and MRI-defined subclinical cerebral infarction: the Atherosclerosis Risk in Communities Study. *Stroke.* 2006;37:82–86.
77. Hughes AD, Falaschetti E, Witt N, et al. Association of retinopathy and retinal microvascular abnormalities with stroke and cerebrovascular disease. *Stroke.* 2016;47:2862–2864.
78. Sairenchi T, Iso H, Yamagishi K, et al. Mild retinopathy is a risk factor for cardiovascular mortality in Japanese with and without hypertension: the Ibaraki Prefectural Health Study. *Circulation.* 2011;124:2502–2511.
79. Wang JJ, Liew G, Klein R, et al. Retinal vessel diameter and cardiovascular mortality: pooled data analysis from two older populations. *Eur Heart J.* 2007;28:1984–1992.
80. McGeechan K, Liew G, Macaskill P, et al. Prediction of incident stroke events based on retinal vessel caliber: a systematic review and individual-participant meta-analysis. *Am J Epidemiol.* 2009;170:1323–1332.
81. McGeechan K, Liew G, Macaskill P, et al. Meta-analysis: retinal vessel caliber and risk for coronary heart disease. *Ann Intern Med.* 2009;151:404–413.
82. Wong TY, Klein R, Nieto FJ, et al. Retinal microvascular abnormalities and 10-year cardiovascular mortality: a population-based case-control study. *Ophthalmology.* 2003;110:933–940.
83. Wang SB, Mitchell P, Liew G, et al. A spectrum of retinal vasculature measures and coronary artery disease. *Atherosclerosis.* 2018;268:215–224.
84. Doubal FN, MacGillivray TJ, Patton N, et al. Fractal analysis of retinal vessels suggests that a distinct vasculopathy causes lacunar stroke. *Neurology.* 2010;74:1102–1107.
85. Kawasaki R, Che Azemin MZ, Kumar DK, et al. Fractal dimension of the retinal vasculature and risk of stroke: a nested case-control study. *Neurology.* 2011;76:1766–1767.
86. Liew G, Mitchell P, Rochtchina E, et al. Fractal analysis of retinal microvasculature and coronary heart disease mortality. *Eur Heart J.* 2011;32:422–429.
87. Yip W, Sabanayagam C, Ong PG, et al. Joint effect of early microvascular damage in the eye & kidney on risk of cardiovascular events. *Sci Rep.* 2016;6:27442.
88. Seidelmann SB, Claggett B, Bravo PE, et al. Retinal vessel calibers in predicting long-term cardiovascular outcomes: the Atherosclerosis Risk in Communities Study. *Circulation.* 2016;134:1328–1338.
89. Keane PA, Sadda SR. Retinal imaging in the twenty-first century: state of the art and future directions. *Ophthalmology.* 2014;121:2489–2500.
90. Swanson E, Huang D. Ophthalmic OCT reaches \$1 billion per year: but reimbursement clampdown clouds future innovation. Available at: <http://www.octnews.org/articles/2844561/ophthalmic-oct-reaches-1-billion-per-year-but-reim/>. Accessed July 20, 2018.
91. Copete S, Flores-Moreno I, Montero JA, et al. Direct comparison of spectral-domain and swept-source OCT in the measurement of choroidal thickness in normal eyes. *Br J Ophthalmol.* 2014;98:334–338.
92. Ramrattan RS, van der Schaft TL, Mooy CM, et al. Morphometric analysis of Bruch's membrane, the choriocapillaris, and the choroid in aging. *Invest Ophthalmol Vis Sci.* 1994;35:2857–2864.
93. Li XQ, Heegaard S, Kilgaard JF, et al. Enhanced-depth imaging optical coherence tomography of the human choroid in vivo compared with histology after enucleation. *Invest Ophthalmol Vis Sci.* 2016;57:371–376.
94. Shao L, Xu L, Chen CX, et al. Reproducibility of subfoveal choroidal thickness measurements with enhanced depth imaging by spectral-domain optical coherence tomography. *Invest Ophthalmol Vis Sci.* 2013;54:230–233.
95. Cameron JR, Ballerini L, Langan C, et al. Modulation of retinal image vasculature analysis to extend utility and provide secondary value from optical coherence tomography imaging. *J Med Imaging (Bellingham).* 2016;3:020501.
96. Balmforth C, van Bragt JJ, Ruijs T, et al. Chorioretinal thinning in chronic kidney disease links to inflammation and endothelial dysfunction. *JCI Insight.* 2016;1:e89173.
97. Wei WB, Xu L, Jonas JB, et al. Subfoveal choroidal thickness: the Beijing Eye Study. *Ophthalmology.* 2013;120:175–180.
98. Kong M, Kwun Y, Sung J, et al. Association between systemic hypertension and macular thickness measured by optical coherence tomography. *Invest Ophthalmol Vis Sci.* 2015;56:2144–2150.
99. Mulè G, Vadalà M, La Blasca T, et al. Association between early-stage chronic kidney disease and reduced choroidal thickness in essential hypertensive patients. *Hypertens Res.* 2019;42:990–1000.
100. Muraoka Y, Tsujikawa A, Kumagai K, et al. Age- and hypertension-dependent changes in retinal vessel diameter and wall thickness: an optical coherence tomography study. *Am J Ophthalmol.* 2013;156:706–714.
101. van Dijk HW, Kok PH, Garvin M, et al. Selective loss of inner retinal layer thickness in type 1 diabetic patients with minimal diabetic retinopathy. *Invest Ophthalmol Vis Sci.* 2009;50:3404–3409.
102. van Dijk HW, Verbraak FD, Kok PH, et al. Early neurodegeneration in the retina of type 2 diabetic patients. *Invest Ophthalmol Vis Sci.* 2012;53:2715–2719.
103. De Clerck EE, Schouten JS, Berendschot TT, et al. New ophthalmologic imaging techniques for detection and monitoring of neurodegenerative changes in diabetes: a systematic review. *Lancet Diabetes Endocrinol.* 2015;3:653–663.
104. Balendra SI, Normando EM, Bloom PA, Cordeiro MF. Advances in retinal ganglion cell imaging. *Eye (Lond).* 2015;29:1260–1269.
105. Querques G, Lattanzio R, Querques L, et al. Enhanced depth imaging optical coherence tomography in type 2 diabetes. *Invest Ophthalmol Vis Sci.* 2012;53:6017–6024.
106. Tavares Ferreira J, Vicente A, Proenca R, et al. Choroidal thickness in diabetic patients without diabetic retinopathy. *Retina.* 2018;38:795–804.
107. Wang JC, Laíns I, Providência J, et al. Diabetic choroidopathy: choroidal vascular density and volume in diabetic retinopathy with swept-source optical coherence tomography. *Am J Ophthalmol.* 2017;184:75–83.
108. Thambirajah J, Landray MJ, McGlynn FJ, et al. Abnormalities of endothelial function in patients with predialysis renal failure. *Heart.* 2000;83:205–209.
109. Stehouwer CDA, Henry RMA, Dekker JM, et al. Microalbuminuria is associated with impaired brachial artery, flow-mediated vasodilation in elderly individuals without and with diabetes: further evidence for a link between microalbuminuria and endothelial dysfunction—the Hoorn Study. *Kidney Int.* 2004;66:S42–S44.
110. Chua J, Chin CWL, Hong J, et al. Impact of hypertension on retinal capillary microvasculature using optical coherence tomographic angiography. *J Hypertens.* 2019;37:572–580.
111. Burton JO, Jefferies HJ, Selby NM, McIntyre CW. Hemodialysis-induced repetitive myocardial injury results in global and segmental reduction in systolic cardiac function. *Clin J Am Soc Nephrol.* 2009;4:1925–1931.
112. Pahor D, Gracner B, Gracner T, Hojs R. [Optical coherence tomography findings in hemodialysis patients]. *Klin Monbl Augenheilkd.* 2008;225:713–717 [in German].
113. Shin YU, Lee SE, Kang MH, et al. Evaluation of changes in choroidal thickness and the choroidal vascularity index after hemodialysis in patients with end-stage renal disease by using swept-source optical coherence tomography. *Medicine.* 2019;98:e15421.
114. Shin YU, Lee DE, Kang MH, et al. Optical coherence tomography angiography analysis of changes in the retina and the choroid after haemodialysis. *Sci Rep.* 2018;8:17184.
115. Zhang Y, Weng H, Li Q, Wang Z. Changes in retina and choroid after haemodialysis assessed using optical coherence tomography angiography. *Clin Exp Optom.* 2018;101:674–679.
116. Chen H, Zhang X, Shen X. Ocular changes during hemodialysis in patients with end-stage renal disease. *BMC Ophthalmol.* 2018;18:208.
117. Chang IB, Lee JH, Kim JS. Changes in choroidal thickness in and outside the macula after hemodialysis in patients with end-stage renal disease. *Retina.* 2017;37:896–905.
118. Ishibazawa A, Nagaoka T, Minami Y, et al. Choroidal thickness evaluation before and after hemodialysis in patients with and without diabetes. *Invest Ophthalmol Vis Sci.* 2015;56:6534–6541.
119. Jung JW, Chin HS, Lee DH, et al. Changes in subfoveal choroidal thickness and choroidal extravascular density by spectral domain

- optical coherence tomography after haemodialysis: a pilot study. *Br J Ophthalmol*. 2014;98:207–212.
120. Yang SJ, Han YH, Song GI, et al. Changes of choroidal thickness, intraocular pressure and other optical coherence tomographic parameters after haemodialysis. *Clin Exp Optom*. 2013;96:494–499.
 121. Ulas F, Dogan U, Keles A, et al. Evaluation of choroidal and retinal thickness measurements using optical coherence tomography in non-diabetic haemodialysis patients. *Int Ophthalmol*. 2013;33:533–539.
 122. Jung JW, Yoon MH, Lee SW, Chin HS. Effect of hemodialysis (HD) on intraocular pressure, ocular surface, and macular change in patients with chronic renal failure: effect of hemodialysis on the ophthalmologic findings. *Graefes Arch Clin Exp Ophthalmol*. 2013;251:153–162.
 123. Theodossiadi PG, Theodoropoulou S, Neamonitou G, et al. Hemodialysis-induced alterations in macular thickness measured by optical coherence tomography in diabetic patients with end-stage renal disease. *Ophthalmologica*. 2012;227:90–94.
 124. Demir MN, Eksioglu U, Altay M, et al. Retinal nerve fiber layer thickness in chronic renal failure without diabetes mellitus. *Eur J Ophthalmol*. 2009;19:1034–1038.
 125. Cheung CY, Ikram MK, Chen C, Wong TY. Imaging retina to study dementia and stroke. *Prog Retin Eye Res*. 2017;57:89–107.
 126. Findlay MD, Dawson J, Dickie DA, et al. Investigating the relationship between cerebral blood flow and cognitive function in hemodialysis patients. *J Am Soc Nephrol*. 2019;30:147–158.
 127. Berindan K, Nemes B, Szabo RP, Modis L Jr. Ophthalmic findings in patients after renal transplantation. *Transplant Proc*. 2017;49:1526–1529.
 128. Altinkaynak H, Kara N, Sayin N, et al. Subfoveal choroidal thickness in patients with chronic heart failure analyzed by spectral-domain optical coherence tomography. *Curr Eye Res*. 2014;39:1123–1128.
 129. Ahmad M, Kaszubski PA, Cobbs L, et al. Choroidal thickness in patients with coronary artery disease. *PLoS One*. 2017;12:e0175691.
 130. Wang J, Jiang J, Zhang Y, et al. Retinal and choroidal vascular changes in coronary heart disease: an optical coherence tomography angiography study. *Biomed Opt Express*. 2019;10:1532–1544.
 131. Arnould L, Seydou A, Gabrielle PH, et al. Subfoveal choroidal thickness, cardiovascular history, and risk factors in the elderly: the Montrachet study. *Invest Ophthalmol Vis Sci*. 2019;60:2431–2437.
 132. Jia Y, Bailey ST, Wilson DJ, et al. Quantitative optical coherence tomography angiography of choroidal neovascularization in age-related macular degeneration. *Ophthalmology*. 2014;121:1435–1444.
 133. Hwang TS, Jia Y, Gao SS, et al. Optical coherence tomography angiography features of diabetic retinopathy. *Retina*. 2015;35:2371–2376.
 134. Vadala M, Castellucci M, Guarrasi G, et al. Retinal and choroidal vasculature changes associated with chronic kidney disease. *Graefes Arch Clin Exp Ophthalmol*. 2019;257:1687–1698.
 135. Sun Z, Tang F, Wong R, et al. OCT angiography metrics predict progression of diabetic retinopathy and development of diabetic macular edema: a prospective study. *Ophthalmology*. 2019;126:1675–1684.
 136. Kim K, Kim ES, Yu SY. Optical coherence tomography angiography analysis of foveal microvascular changes and inner retinal layer thinning in patients with diabetes. *Br J Ophthalmol*. 2018;102:1226–1231.
 137. Sohn EH, van Dijk HW, Jiao C, et al. Retinal neurodegeneration may precede microvascular changes characteristic of diabetic retinopathy in diabetes mellitus. *Proc Natl Acad Sci U S A*. 2016;113:2655–2664.
 138. Alicic RZ, Rooney MT, Tuttle KR. Diabetic kidney disease: challenges, progress, and possibilities. *Clin J Am Soc Nephrol*. 2017;12:2032–2045.
 139. Cheung CY, Tang F, Ng DS, et al. The relationship of quantitative retinal capillary network to kidney function in type 2 diabetes. *Am J Kidney Dis*. 2018;71:916–918.
 140. Chawla LS, Amdur RL, Amodeo S, et al. The severity of acute kidney injury predicts progression to chronic kidney disease. *Kidney Int*. 2011;79:1361–1369.
 141. Odutayo A, Wong CX, Farkouh M, et al. AKI and long-term risk for cardiovascular events and mortality. *J Am Soc Nephrol*. 2017;28:377–387.
 142. Alan G, Guenancia C, Arnould L, et al. Retinal vascular density as a novel biomarker of acute renal injury after acute coronary syndrome. *Sci Rep*. 2019;9:8060.
 143. Arnould L, Guenancia C, Azemar A, et al. The Eye-MI pilot study: a prospective acute coronary syndrome cohort evaluated with retinal optical coherence tomography angiography. *Invest Ophthalmol Vis Sci*. 2018;59:4299–4306.
 144. Martens RJH, Houben A, Kooman JP, et al. Microvascular endothelial dysfunction is associated with albuminuria: the Maastricht Study. *J Hypertens*. 2018;36:1178–1187.
 145. Sorensen BM, Houben AJ, Berendschot TT, et al. Prediabetes and type 2 diabetes are associated with generalized microvascular dysfunction: the Maastricht Study. *Circulation*. 2016;134:1339–1352.
 146. Delles C, Michelson G, Harazny J, et al. Impaired endothelial function of the retinal vasculature in hypertensive patients. *Stroke*. 2004;35:1289–1293.
 147. Bruckmann A, Seeliger C, Lehmann T, et al. Altered retinal flicker response indicates microvascular dysfunction in women with preeclampsia. *Hypertension*. 2015;66:900–905.
 148. Nägele MP, Barthelmes J, Ludovici V, et al. Retinal microvascular dysfunction in hypercholesterolemia. *J Clin Lipidol*. 2018;12:1523–1531. e1522.
 149. Nägele MP, Barthelmes J, Ludovici V, et al. Retinal microvascular dysfunction in heart failure. *Eur Heart J*. 2018;39:47–56.
 150. Zhi Z, Chao JR, Wietcha T, et al. Noninvasive imaging of retinal morphology and microvasculature in obese mice using optical coherence tomography and optical microangiography. *Invest Ophthalmol Vis Sci*. 2014;55:1024–1030.
 151. Patel PJ, Foster PJ, Grossi CM, et al. Spectral-domain optical coherence tomography imaging in 67 321 adults: associations with macular thickness in the UK Biobank study. *Ophthalmology*. 2016;123:829–840.
 152. McCormick E. OCT rollout in every Specsavers announced. Available at: <https://www.Aop.Org.Uk/ot/industry/high-street/2017/05/22/oct-rollout-in-every-specsavers-announced>. Accessed July 20, 2018.
 153. LeCun Y, Bengio Y, Hinton G. Deep learning. *Nature*. 2015;521:436–444.
 154. Gulshan V, Peng L, Coram M, et al. Development and validation of a deep learning algorithm for detection of diabetic retinopathy in retinal fundus photographs. *JAMA*. 2016;316:2402–2410.
 155. Poplin R, Varadarajan AV, Blumer K, et al. Prediction of cardiovascular risk factors from retinal fundus photographs via deep learning. *Nat Biomed Eng*. 2018;2:158–164.
 156. De Fauw J, Ledsam JR, Romera-Paredes B, et al. Clinically applicable deep learning for diagnosis and referral in retinal disease. *Nat Med*. 2018;24:1342–1350.
 157. Giani A, Cigada M, Choudhry N, et al. Reproducibility of retinal thickness measurements on normal and pathologic eyes by different optical coherence tomography instruments. *Am J Ophthalmol*. 2010;150:815–824.
 158. Corvi F, Pellegrini M, Erba S, et al. Reproducibility of vessel density, fractal dimension, and foveal avascular zone using 7 different optical coherence tomography angiography devices. *Am J Ophthalmol*. 2018;186:25–31.